Energy Conversion & Storage Program

1993 Annual Report

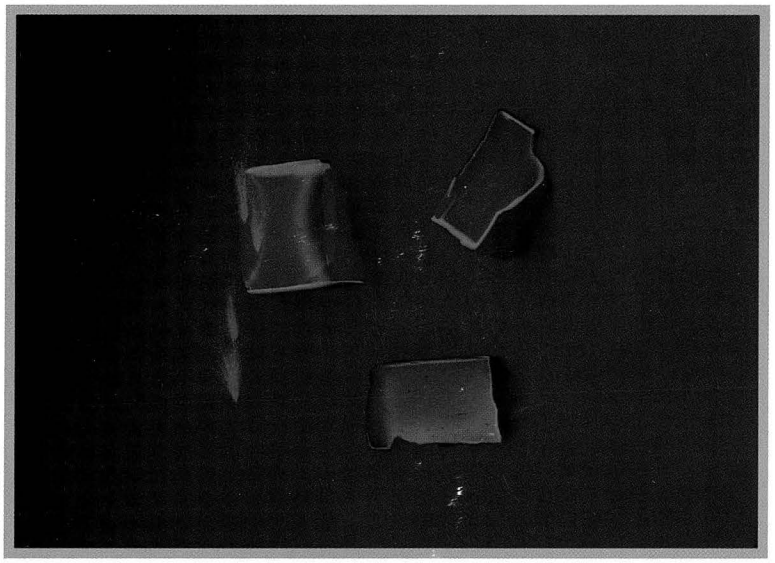

LBL-35242
Copy 2
| LOAN COPY |
|Circulates |
|for 4 weeks| Bldg. 50 Library.

Energy & Environment Di
Lawrence Berkeley Labc
UNIVERSITY OF CALI

LBL-35242
UC-350
June 1994

Available to DOE and DOE Contractors from
Office of Scientific and Technical Information
P.O. Box 62, Oak Ridge, TN 37831
Prices available from (615) 576-8401

Available to the public from
National Technical Information Service
U.S. Department of Commerce
5285 Port Royal Road, Springfield, VA 22161

Prepared for the U.S. Department of Energy under Contract No. DE-AC03-76SF00098

DISCLAIMER

This document was prepared as an account of work sponsored by the United States Government. While this document is believed to contain correct information, neither the United States Government nor any agency thereof, nor the Regents of the University of California, nor any of their employees, makes any warranty, express or implied, or assumes any legal responsibility for the accuracy, completeness, or usefulness of any information, apparatus, product, or process disclosed, or represents that its use would not infringe privately owned rights. Reference herein to any specific commercial product, process, or service by its trade name, trademark, manufacturer, or otherwise, does not necessarily constitute or imply its endorsement, recommendation, or favoring by the United States Government or any agency thereof, or the Regents of the University of California. The views and opinions of authors expressed herein do not necessarily state or reflect those of the United States Government or any agency thereof or the Regents of the University of California.

Energy Conversion & Storage Program 1993 Annual Report

Elton J. Cairns, Program Head

Energy & Environment Division
Lawrence Berkeley Laboratory
University of California
Berkeley, California 94720
(510) 486-5001

Report No. LBL-35242

Contents

Introduction

Electrochemistry

Exploratory Technology Research Program for Electrochemical Energy Storage 1
Advanced Electrode Research 3
Electrode Surface Layers 7
EXAFS Studies of Electrode Materials for Lithium Batteries 8
Application of Pulsed Laser Deposition to the Study of Rechargeable Battery Materials 9
Fundamental Characterization of Carbon-Based Materials for Electrochemical Systems 9
Applied Research on Lithium/Polymer-Electrolyte Cells 9

Chemical Applications

High-Temperature H_2S-Removal and Sulfur-Recovery Processes 10
Separations by Reversible Chemical Complexation 13
X-Ray Absorption Spectroscopy of Metalloproteins and Related Systems 14
Fundamental Studies of Laser-Material Interactions 15
Photothermal Deflection Spectroscopy of Uranium Oxidation and Dissolution 16
Sensors for Remote Monitoring 17
Bioorganometallic Chemistry: Bonding Studies of a (η^5-pentamethylcyclopentadienyl)rhodium Aqua Complex to Nucleobases, Nucleotides, and Sequence-Specific Oligonucleotides for Human Genome Applications 18
Removal and Recovery of Toxic Metal Ions from Aqueous Streams by Use of Polymer Pendant Ligands 19

Material Applications

Development of New Composite Aerogel Materials 19
Modeling Light Scattering from Nonspherical Microorganisms in the Ocean 20
Mueller Matrix Measurements of Sea Ice 21

Introduction

The Energy Conversion and Storage Program applies chemistry and materials science principles to solve problems in

- production of new synthetic fuels;
- development of high-performance rechargeable batteries and fuel cells;
- development of high-efficiency thermochemical processes for energy conversion;
- characterization of complex chemical processes and chemical species;
- the study and application of novel materials for energy conversion and transmission.

Projects focus on transport-process principles, chemical kinetics, thermodynamics, separation processes, organic and physical chemistry, novel materials, and advanced methods of analysis.

Electrochemistry research aims to develop advanced power systems for electric vehicle and stationary energy storage applications. Topics include the exploratory development of new electrochemical couples for advanced rechargeable batteries, improvements in battery and fuel-cell materials, the establishment of engineering principles applicable to electrochemical energy storage and conversion, and the characterization of lithium/polymer-electrolyte cells for the U.S. Advanced Battery Consortium.

Chemical Applications research includes topics such as separations, catalysis, fuels, and chemical analyses. Included in this program area are projects to develop improved, energy-efficient methods for processing product and waste streams from synfuel plants, coal gasifiers and biomass conversion processes. Of particular interest are new techniques to remove compounds such as H_2S, NH_3 and phenols from effluents, and to devise energy-efficient means for product recovery. Also of current interest is the use of advanced organometallic catalysts to produce bio-organic compounds needed for Human Genome studies. X-ray absorption spectroscopy is being used to characterize chemical systems, and ultrasensitive spectroscopies are being adapted for chemical analyses of trace amounts of rare-earth and actinide compounds.

Materials Applications research includes the evaluation of the properties of advanced materials, as well as the development of novel preparation techniques. For example, techniques such as sputtering, laser ablation and pulsed laser deposition are being used to produce high-temperature super-conducting films. Sol-gel and solvent-extraction methods are used to produce aerogel superinsulators; and light-scattering techniques are being adapted to characterize sea water and sea ice in order to better interpret remote (*e.g.*, satellite) observations of the surface of the earth.

Program Staff

Elton J. Cairns, *Head*
Richard Russo, *Deputy Head*
Harvey Blanch, *Deputy Head*

Thomas Adler
Paul Berdahl
Edério Bidóia
Harvey Blanch
Robert Broekhuis
Garth Burns
Wanqing Cao
Van Carey
Wing-Tat Chan
Jie Chan
Yohan Choi
Douglas Clark
Douglas Coen
Stephen Cramer
Amy Eccles
Laurent Fenouil
Richard Fish
Hubert Gasteiger
Melissa Grush
Craig Horne
Ming-Cheng Hsiao
Songping Huang
Arlon Hunt
Mary Hunt
Jacob Jorné
Jordan Kahn
Marvin Kilgo
C. Judson King
Kimio Kinoshita
Gregory Klunder
Karen Koigawachi
Fanping Kong
Susan Lauer
Daehee Lee
Jane Lee
Yongsik Lee
Wei Li
Scott Lynn
Xianglei Mao
Daniel Mayeri
Frank McLarnon
David Miller
Jeffrey Moore
Marek Odziemkowski
Robert Plivelich
Clayton Randall
Ronald Reade
James Rudnicki
Richard Russo
Robert Selleck
Mark Shannon
Daniel Shapiro
XiangYun Song
Jonathan Spear
Charlotte Standish
Peter Stevens
Kathryn Striebel
Waltraud Taucher
Jerome Thomas
Gavin Towler
Lisa Tung
Jan van Elp
Hongxin Wang
Xin Wang
Charles Wilke
Chin-On Wong
Mark Yahnke
Shouquan Zeng

Electrochemistry

Exploratory Technology Research Program for Electrochemical Energy Storage

E.J. Cairns, K. Kinoshita, F.R. McLarnon

Lawrence Berkeley Laboratory (LBL) is lead center for management of the Exploratory Technology Research (ETR) Program, which is supported by the Electric/Hybrid Propulsion Division of DOE's Office of Transportation Technologies. This program's research supports DOE development of electrochemical energy conversion systems for potential use in electric vehicles. The most-promising electrochemical technologies are identified and transferred to the U.S. Advanced Battery Consortium (USABC) and/or to another DOE program for further development and scale-up.

The ETR Program identifies new electrochemical couples for advanced batteries, determines the technical feasibility of the new couples, improves battery components and materials, establishes engineering principles applicable to electrochemical energy storage and conversion, and investigates fuel cell and metal/air systems for transportation applications. Major emphasis is given to applied research that will lead to superior performance and lower life-cycle costs.

The LBL senior investigators participating in the project are E.J. Cairns, K. Kinoshita, and F.R. McLarnon of the Energy and Environment Division; and L.C. DeJonghe, J.W. Evans, J.S. Newman, P.N. Ross, and C.W. Tobias of the Materials Sciences Division. Research projects conducted by subcontractors are described in the recent annual report, Exploratory Technology Research Program for Electrochemical Energy Storage (LBL-34081); LBL in-house work is summarized in the next article and in the Materials Sciences Division 1993 Annual Report. Highlights of the ETR Program subcontracted work follow.

Exploratory Research

A subcontract was awarded to the Advanced Energy Systems Division of Acme Electric Corporation on the basis of a Request-for-Proposals to extend the development of advanced Zn/NiOOH cell technology. The objectives of this project are to evaluate the LBL family of ternary electrolytes for extending the cycle life of large-size Zn/NiOOH cells and to develop Zn/NiOOH battery technology for EV applications. Early cycles of cells containing sintered NiOOH positive/plastic-bonded Zn negative or fiber-bonded NiOOH positive/plastic-bonded Zn negative showed that good cell capacities can be obtained, but indicate that some technical issues must be resolved to achieve the excellent cycle-life performance obtained at LBL in small-size cells.

Applied Science Research

Research projects at the Illinois Institute of Technology (IIT) and the Environmental Research Institute of Michigan (ERIM) are underway to develop corrosion-resistant materials for use in high-temperature batteries, such as Na/S and Li/FeS_2. IIT is evaluating the quality of Mo_2C coatings obtained by plasma-enhanced chemical vapor deposi tion. X-ray photoelectron spectroscopy (XPS) analysis indicated that the films deposited on a glass or steel substrate contain a significant fraction of oxygen. The use of hydrogen and methane as a carrier gas is being evaluated to minimize the oxygen activity in the reaction chamber. ERIM has prepared TiN-coated Al containment materials by sputter-deposition techniques for corrosion testing in molten Na_2S_4 at 350°C. After three weeks in the polysulfide melt a conductive surface film was still present on the sample coated with TiN. Final analyses of the physicochemical properties of the coating have not been completed.

Brookhaven National Laboratory (BNL) has used extended x-ray absorption fine structure (EXAFS) and x-ray absorption near-edge spectroscopy (XANES) to study manganese oxide compounds, Bi-doped manganese oxide and Li_xMnO_2. These materials are under consideration for use in rechargeable Zn and Li cells, but have not been well characterized. EXAFS data were obtained at both the Mn K edge and the BiL_3 edge for Bi-doped manganese oxide that was discharged in 9 M KOH. At the end of the one-electron discharge the manganese oxide is highly disordered, whereas on completion of the two-electron discharge, the product reverts back to an ordered phase.

Case Western Reserve University (CWRU) has used *in situ* spectroscopic techniques and thermal analysis to study the Li/organic electrolyte interface. It is of critical importance to understand the complex interfacial phenomena in Li batteries, because such phenomena limit the life and performance of rechargeable Li cells. XPS studies indicated that the interactions between Li and perdeuterated tetrahydrofuran (TDF) are strong, leading to substantial structural modifications. Thermal desorption studies with TDF revealed that Li can dehydrogenate TDF to form LiD as one of the predominant products. This type of information is needed to develop a Li electrode/electrolyte combination that

exhibits reversible behavior. CWRU is utilizing *in situ* EXAFS and XANES spectroscopies to investigate electrochemical phenomena in Li/FeS_2 cells. Initial effort has centered on studies of Li/FeS_2 cells that operate at room temperature. During discharge Li is inserted into FeS_2, and the corresponding EXAFS spectra revealed a gradual loss in the fine structure as the amount of Li is increased.

Johns Hopkins University has extended the studies on the passivation and anodic behavior of iron and 1018 carbon steel in $LiAsF_6$/dimethoxyethane (DME). This information is needed to determine the stability limits of materials of construction for Li batteries. In a nominally dry $LiAsF_6$/DME solution containing 50-100 ppm H_2O, the dissolution of Fe and the electropolymerization of the DME solvent are believed to play major roles in the repassivation mechanism. In addition, the electropolymerization reaction is dependent on the presence of $LiAsF_6$; no polymerization is observed in its absence or when other salts are present instead.

Air Systems Research

CWRU has completed an extensive 8-year (1984-1992) study of oxygen electrocatalysis on various transition-metal macrocycles and oxide catalysts. This effort resulted in a better understanding of O_2 reduction and evolution on these electrocatalysts in acidic and alkaline electrolytes. The significant accomplishments of the research were summarized in a report (LBL-33814).

Eltech Research Corporation is investigating the viability of graphitized carbon blacks and metal oxides as electrocatalyst supports in bifunctional air electrodes for electrically rechargeable Zn/air cells. Graphitized carbon blacks of both Monarch 120 and Shawinigan acetylene black appear to be suitable electrocatalyst supports. Electrochemical tests of $NiCo_2O_4$/Monarch 120 in small cells at MATSI, Inc. achieved over 350 cycles.

Los Alamos National Laboratory (LANL) has found that processing membrane-electrode assemblies (MEA) with Nafion membranes that contain tetrabutyl ammonium are more robust than those obtained from the Na^+ and H^+ forms. Life tests of up to 4000 h have been achieved by LANL with only a 10% performance loss using membrane/electrode assemblies with thin-layer catalyst layers in polymer electrolyte fuel cells (PEFCs) at 80°C. A new membrane from DuPont (Nafion 5L) was evaluated that showed a protonic conductivity of about 20% higher than that for Nafion 117. Its water uptake was about twice that of Nafion 117, membrane C, and an experimental Dow membrane. The influence of CO_2 on the performance of anodes in PEFCs was investigated. The study showed that the reverse shift reaction involving CO_2, and the electrochemical reduction of CO_2, both produce CO which poisons the anode. Permeation of CH_3OH through Nafion in PEFCs was studied by LANL. Permeation rates equivalent to 200 mA/cm^2 were determined with 45% CH_3OH in the fuel stream.

BNL is utilizing x-ray absorption spectroscopy (XAS) to study the correlation between the electronic properties of carbon-supported Pt/Cr, Pt/Co and Pt/Ni alloy catalysts and their electrocatalytic activity for oxygen reduction. The results indicate that alloying Pt enhances the performance of the oxygen electrode in a PEM fuel cell.

Future Directions

LBL renewed its Cooperative Research and Development Agreement (CRADA) with the USABC to develop advanced Li/polymer-electrolyte batteries for electric vehicles. Research on the CRADA involves investigators from both the Energy and Environment and Materials Science Divisions. Effort is underway on tasks to study electrochemical phenomena at Li/polymer interfaces, develop mathematical modeling of Li/polymer cells, synthesize improved polymer electrolytes and materials for positive electrodes, establish a bibliographic database on components for Li/polymer cells, and investigate overcharge/overdischarge phenomena in secondary Li cells. LBL, in collaboration with EPRI, issued a request for proposals on "Applied Research on Novel Components for Advanced Secondary Batteries." A total of 39 proposals were received, and nine were selected for funding. EPRI is supporting a project at the Georgia Institute of Technology, and LBL is supporting new projects at Northwestern University (2), Case Western Reserve University, SRI International, PolyPlus Battery Co. Inc., Rutgers University, State University of New York at Binghamton, and University of Dayton. The overall theme of this new research thrust is to develop novel materials that will lead to high-performance Li batteries with the potential to meet long-term USABC battery performance goals.

References

Kinoshita K, *et al.* *Exploratory technology research program for electrochemical energy storage: Annual report for 1992.* Lawrence Berkeley Laboratory Report No. LBL-34081, October 1993.

McLarnon FR, Kinoshita K, Cairns EJ. Overview of the exploratory technology research program. In: *Preprints of the Annual Automotive Technology Development Contractors' Coordination Meeting*, Vol. II, Dearborn, MI, October 1993.

Cairns EJ, McLarnon F.R. Status of batteries for energy storage applications. *Proceedings of the Symposium on Batteries and Fuel Cells for Stationary and Electric Vehicle Applications.* Landgrebe AR and Takehara Z, eds. Pennington NJ: The Electrochemical Society, 1993; 93-8: 1-11.

McLarnon FR. Electric battery research. Paper presented at the Supercities International Conference on the Environment, San Francisco, CA, October 1992.

Cairns EJ, McLarnon FR. Status of batteries for energy storage applications. Paper No. 21, 183rd Meeting of the Electrochemical Society, Honolulu, HI, May 1993.

Advanced Electrode Research

E.J. Cairns, F.R. McLarnon, T.C. Adler, E. Bidóia†, Y. Choi, H.A. Gasteiger, M.-C. Hsiao†, J. Jorné†, J.A. Reimer*, R.F. Plivelich, P.N. Ross*, K.A. Striebel, W. Taucher†, C. Wong, M.S. Yahnke

We have been studying the behavior of electrodes used in advanced secondary batteries and fuel cells currently under development for energy storage applications. In addition, we have been investigating practical means for improving the performance and lifetimes of these batteries and fuel cells. Systems of current interest include ambient-temperature, alkaline-electrolyte rechargeable cells with Zn electrodes (Zn/NiOOH, Zn/air), and fuel cells that utilize the direct electrooxidation of methanol fuel. We study life-limiting and performance-limiting phenomena under realistic cell operating conditions.

Investigations of Methods to Improve the Lifetime of the Zinc/Nickel Oxide Cell

Rechargeable alkaline Zn/NiOOH cells can be designed to deliver high specific energy and high specific power, but their short lifetimes have precluded commercial acceptance. The high solubility of Zn species in 7M KOH alkaline electrolytes tends to enhance unwanted Zn active material redistribution (shape change) which degrades cell capacity and limits its life. Our earlier work demonstrated that KOH-KF-K_2CO_3 electrolytes greatly extend the cycle life of 1.35-Ah Zn/NiOOH cells. We use 3-5M KOH concentrations, which result in much lower Zn species solubility. The F^- and CO_3^{2-} additions (~2M each) not only increase the electrolyte ionic conductivity, but may also influence the kinetics of Zn deposition and dissolution (see next section). The rate of Zn-electrode shape change is much slower in these cells, and cell cycle life is increased to 500-800 deep-discharge cycles, compared to 100-200 cycles in traditional 7M KOH - 0.5M LiOH electrolytes. Zn/NiOOH cells employing these novel electrolytes now tend to be life-limited and performance-limited by the NiOOH electrode rather than the Zn electrode. We have therefore placed increased emphasis on improving NiOOH electrode performance without compromising the excellent lifetime of the Zn electrode.

We evaluated various types of NiOOH electrodes in KOH-KF-K_2CO_3 electrolytes by cycling pairs of NiOOH electrodes to assess electrode performance without the complicating effects of a Zn electrode. The NiOOH electrodes employed sintered-Ni plaque, Ni-plated plastic fiber, and Ni foam-metal current collectors. The KOH concentration was varied from 3M to 6M, and F^- and CO_3^{2-} ionic concentrations were fixed at 2M. Increasing the KOH concentration above 4.5M afforded no improvement in NiOOH electrode capacity. All NiOOH electrodes suffered a 10-20% decrease in capacity when the electrolyte was saturated with ZnO, which is consistent with the results of prior Zn/NiOOH cell cycle-life tests.

Lithium hydroxide is traditionally added to KOH electrolyte to promote efficient operation of the NiOOH electrode in rechargeable alkaline batteries. Fluoride ions in the KOH-KF-K_2CO_3 electrolyte precipitated any added Li^+ ion as insoluble LiF, which prevents the Li^+ from reaching the interior pores of the NiOOH electrode and results in a ~10% decrease in electrode capacity. We have developed a novel technique for preparing a very fine suspension of LiF particles, which when added to KOH-KF-K_2CO_3 electrolytes result in a full recovery to the expected NiOOH electrode capacity. Life-cycle testing is underway to define an upper limit for KOH concentration and lower limits for F^- and CO_3^{2-} ionic concentrations that result in improved lifetimes of Zn/NiOOH cells.

Zinc/nickel oxide cells with traditional 7M KOH - 0.5M LiOH electrolytes exhibit very high peak specific power (>400 W/kg) early in cell life, but the peak power declines rapidly with repeated charge-discharge cycling. Similar cells with KOH-KF-K_2CO_3 electrolytes deliver a peak specific power of >300 W/kg at 0% DOD and >200 W/kg at 80% DOD; however, this peak power level is retained throughout the cell lifetime. High specific energy, high specific power, low cost, low toxicity, and extended lifetime make this new Zn/NiOOH technology attractive for use in electric vehicles and portable electronic devices. Many battery manufacturers from all parts of the world visit LBL on a regular basis to learn about this exciting new version of an old battery technology. During 1993 we worked closely with Acme Advanced Energy Systems (Tempe, AZ) to help develop and scale-up this promising technology.

Investigation of Zinc Species Precipitation in Nickel Electrodes

Our recent improvements in the cycle-life performance of the Zn electrode in rechargeable Zn/NiOOH cells demonstrated that the NiOOH electrode now limits cell lifetimes. We have used various techniques to characterize NiOOH electrodes recovered from Zn/NiOOH cells cycled using the novel low-zinc-solubility electrolytes described above, in an effort to better define the reason(s) for the gradual capacity loss we observed in these cells. X-ray photo-

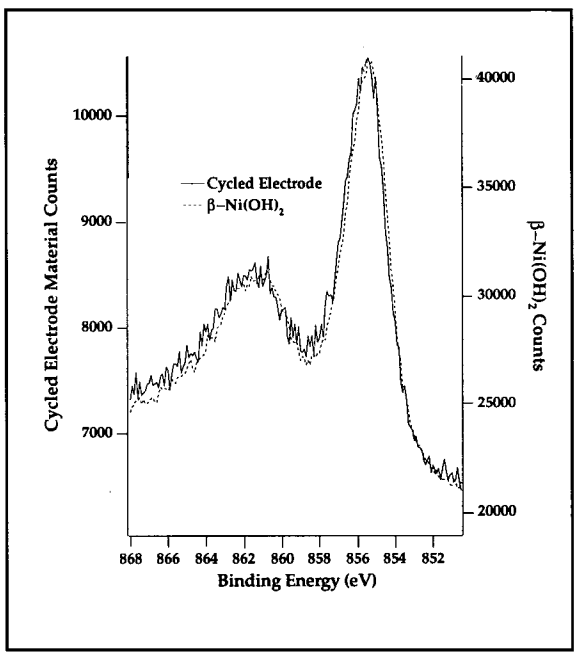

Fig. 1. *Comparison of the photoelectron spectrum of a porous NiOOH electrode harvested from a Zn/NiOOH cell with that of chemically prepared β–Ni(OH)₂.*

*Materials Sciences Division, LBL
†Visiting scientist

electron spectroscopy (XPS), vibrational spectroscopies (IR and Raman) and x-ray diffraction techniques were used to determine the chemical composition of Ni and Zn species in cycled NiOOH electrodes. Only XPS gave high-quality results. Advantages of XPS include its elemental specificity, surface specificity, and ability to identify differing chemical "states" of a given element. Previous investigators have postulated that ZnO may precipitate and block the NiOOH electrode surface, or that Zn may react with the Ni active material and produce an electrochemically inactive Ni-Zn compound. Figure 1 compares the Ni $2p_{3/2}$ XPS spectrum of a discharged NiOOH electrode cycled in 3.5M KOH - 2M K_2CO_3 - 2M KF electrolyte with that of chemically prepared β-$Ni(OH)_2$. The spectra substantially agree with each other, which suggests that the NiOOH electrode does not chemically react with Zn species under cell-cycling conditions. Similar experiments indicated that the Ni $2p_{3/2}$ spectrum of discharged NiOOH electrode material cycled in 3.5M KOH - 2M K_2CO_3 - 2M KF electrolyte agreed with the spectrum of discharged NiOOH material cycled in 6M KOH - 1M LiOH electrolyte, which suggests that CO_3^{2-} and F^- species do not react with Ni under cell-cycling conditions. Measured Zn spectra indicated that the Zn deposited in cycled NiOOH electrodes is in the form of ZnO.

We also considered the possibility that various chemical or mechanical processes may degrade the sintered-Ni current collector, leading to loss of electronic contact and poor utilization of the NiOOH active material. Four-point conductivity measurements were carried out on various NiOOH-electrode samples harvested from a 21-Ah Zn/NiOOH cell which was subjected to 200 deep-discharge cycles. The measured resistivity varied significantly with position in the cycled NiOOH electrodes, which implies that a mechanical degradation process is at least partially responsible for electrode capacity decline.

Planned work will clarify the relative importance of various processes occurring in the NiOOH electrode that are suspected of causing capacity degradation. The general strategy will be to modify cycled NiOOH electrodes in ways that will eliminate or reduce the importance of various capacity-degradation modes, and attempt to recover lost capacity.

Influence of K_2CO_3 Additions on the Kinetics of the Zinc Electrode in Alkaline Electrolyte

Our prior studies have shown that additives such as K_2CO_3 and KF have a major effect on the rate and extent of Zn active material redistribution during cell cycling experiments. These beneficial effects cannot be attributed solely to the reduction of Zn species solubility that is associated with lower KOH concentration in these electrolytes. We have carried out steady-state and potential-step polarization measurements to characterize the behavior of Zn-electrode reactions in alkaline electrolytes with and without K_2CO_3 additions. The objective of these studies is to determine if the beneficial effect of the K_2CO_3 additions is associated with fundamental changes in the Zn-electrode kinetics.

Because the Zn electrode is always covered by an oxidized surface layer in alkaline electrolytes, it is critically important to establish a reliable electrode pretreatment procedure to obtain reproducible electrode surface conditions. We demonstrated that reproducible Zn electrode surfaces can be achieved by using a square-wave potential pulse (-5 mV cathodic polarization for 60 sec followed by holding the Zn electrode at its rest potential for 60s) pretreatment procedure. Figure 2 shows typical steady-state polarization curves for the Zn electrode in 2.5M KOH - 0.15M ZnO electrolytes with and without the addition of 2.5M K_2CO_3. The current densities in the carbonate-containing electrolyte are generally lower than those in the carbonate-free electrolyte, as is the derived exchange current density. The region of low over potentials (<10mV) is of greatest interest in this study, because that is the region wherein practical battery electrodes operate. We have measured the transient current response to potential steps in this region, and we are developing a phenomenological model to describe the detailed mechanisms of the Zn-electrode reaction in these electrolytes. In our model, a chemical reaction step is followed by two consecutive charge-transfer reactions on the Zn electrode surface in the presence of a porous surface layer.

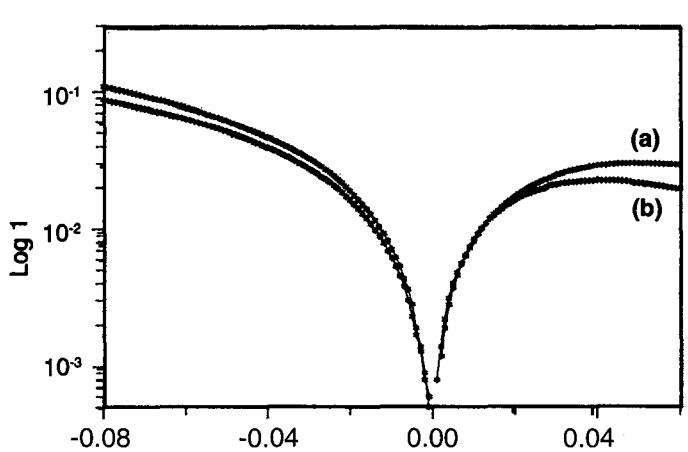

Fig. 2. *Polarization curves for Zn electrodes in alkaline electrolyte. The ordinate is the absolute value of the current density (A cm^{-2}) and the abscissa is the electrode potential measured against another Zn electrode at its rest potential. The curves show the current-potential response for a Zn electrode in 2.5M KOH - 0.15M ZnO electrolyte (a) without and (b) with the addition of 2.5M K_2CO_3.*

Evaluation of Zinc/Air Cells

We have performed cycle-life tests of Zn/air cells with several configurations of Zn electrode (flowing soluble Zn and pasted insoluble Zn) paired with commercially available bifunctional (*i.e.*, catalyzes both the reduction and evolution of O_2) air electrodes from Westinghouse Electric Co. and Eltech Systems Inc. The soluble Zn electrode, with forced convection, exhibits extremely low polarization even at high current densities. The quality and location of the Zn deposit depend

strongly on the direction of flow. When flow is directed toward the air electrode the Zn deposit grows out of the foam substrate toward the air electrode. The best configuration, from the standpoint of minimum system complexity and ohmic loss, is that with the flow parallel with the face of the electrode, as previously used.

Several experimental bifunctional air electrodes from Westinghouse were evaluated in a specially designed flow cell. Electrodes constructed with graphitized Black Pearls carbon showed extremely high corrosion rates as indicated by severe discoloration of the electrolyte after a few cycles. The polarization behavior of these electrodes was not affected, probably because we used highly alkaline electrolytes (45% KOH) with the soluble Zn electrodes; however, the current efficiency on the Zn electrode was limited to low values.

Pasted Zn electrodes were cycled with both Eltech air electrodes and Westinghouse air electrodes based on Shawinigan Black carbon. Neither of these air electrodes corroded as rapidly as those mentioned above. These cells were cycled with 3.5M KOH - 2M K_2CO_3 - 2M KF electrolyte, both at 33% utilization of the Zn material and at a higher utilization corresponding to a Zn electrode cutoff potential of -1.0V (*vs* Hg/HgO). Zinc electrode performance at 33% utilization compared quite well with that observed in Zn/NiOOH cells using the same electrolyte. At higher utilization, the Zn electrode coulombic efficiency was significantly lower.

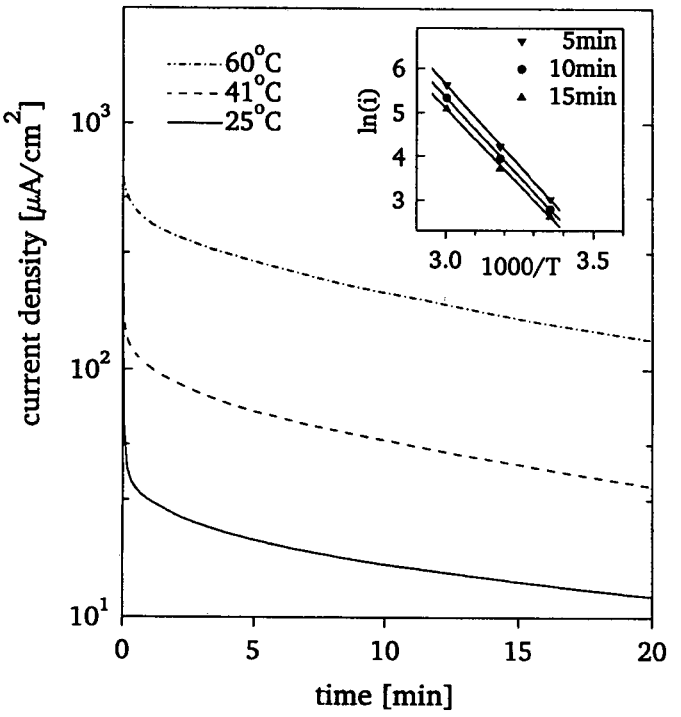

Fig. 3. *Transient CH_3OH oxidation current densities recorded at various temperatures. The inset illustrates the Arrhenius-type behavior of these data.*

Effect of Electrocatalyst and Electrolyte Composition on Methanol/Air Fuel-Cell Performance

Fuel cells offer the promise of higher energy conversion efficiency and greatly reduced emissions, compared to combustion engines, and they are being developed for use in electric vehicles. However, present-day fuel cells operate on H_2, so either a H_2-storage device or a reformer must be carried on-board the vehicle. Each of these H_2-delivery options results in a heavy, bulky, costly, slow-reacting, and complex fuel-cell power plant. There is a strong need to develop a fuel cell that can electrochemically oxidize liquid fuels, and the successful development of a direct-methanol fuel cell (DMFC) would represent a major advance for fuel-cell-powered vehicles. However, some major obstacles must be addressed before acceptable performance can be attained with DMFCs. The oxidation rate of CH_3OH is several orders of mag-nitude lower than that of H_2 on a Pt catalyst, and oxidation products other than the expected H_2O and CO_2 were observed in some cases. The problem of the slow oxidation rate of CH_3OH has been partially addressed by utilizing bimetallic catalysts (see next section). Previous work in this laboratory has confirmed that a Pt/Ru catalyst supported on graphitized carbon has a significantly higher catalytic activity for the oxidation of CH_3OH than supported Pt alone.

Cathode deactivation and the formation of CH_2O in acidic electrolytes, and the unwanted formation of carbonates in alkaline electrolytes, have prompted previous researchers to study buffered electrolytes. Aqueous Cs_2CO_3 appears to be an electrolyte that does not suffer from the shortcomings of acidic and other alkaline electrolytes. The major goal of this research project is to demonstrate in a realistic system that the electrooxidation of CH_3OH is efficient and produces only H_2O and CO_2 as reaction products. A model fuel cell was designed and fabricated to accommodate 20-cm² electrodes. Fuel cell polarization tests using H_2 feed and H_2SO_4 electrolyte are under way; the results of these tests will serve to calibrate the fuel cell. Future experiments will seek to optimize DMFC performance by varying catalyst composition and electrode structure. Analyses of the electrolyte and exit gases will be performed to determine if CH_3OH oxidizes completely to benign reaction products. An examination of an optimized system will be performed to ascertain its suitability for electric vehicles and other applications.

Methanol Electrooxidation on Well-Characterized Platinum-Ruthenium Alloys

The electrooxidation of CH_3OH in H_2SO_4 electrolyte on well-characterized Pt-Ru alloy electrodes was studied over the temperature range from 25-60°C. The relationship between the bulk and surface compositions of annealed and sputter-cleaned alloy electrodes was determined definitively in ultra-high vacuum (UHV) *via* low-energy ion scattering (LEIS) and Auger electron spectroscopy (AES). Equilibrated, *i.e.*, annealed, alloy surfaces were strongly enriched in Pt, consistent with ideal solution thermodynamics, whereas the non-equilibrium process of sputtering

produced surfaces which closely resembled the bulk structures of the alloys. The rate-limiting step in the electrooxidation of CH_3OH on sputter-cleaned Pt-Ru electrodes at 25°C was shown to be the initial adsorption/dehydrogenation of CH_3OH on Pt surface atom ensembles, resulting in an optimum Ru surface composition of ~10 at%; conversely, Ru-rich surfaces retard the CH_3OH oxidation reaction because Ru is inactive towards the dissociative adsorption of CH_3OH. However, the nucleation of O_2-containing species on bare Ru atoms at low electrode potentials promotes the oxidative removal of CH_3OH dehydrogenation fragments, thereby preventing the long-term deactivation of Pt-Ru electrodes. This bifunctional character of Pt-Ru alloys was verified in measurements of their electrocatalytic activity toward the electrooxidation of CO. The nucleation of O_2-containing species on Ru surface atoms significantly enhanced the oxidation rate of adsorbed CO, producing a catalytic shift of 0.25V for an alloy with the optimum Ru surface composition of ~50 at%. The same optimum Ru surface composition was observed in the electrooxidation of HCOOH, which similar to CO interacts with both Pt and Ru surface atoms. For the CH_3OH electrooxidation reaction it was found that the activity of Ru toward the dissociative adsorption of CH_3OH is a strong function of temperature. This change in the adsorptive nature of the Ru sites with temperature produced a variation in the optimum surface composition with temperature, from ~10 at% at 25°C to ~30 at% at 60°C. The shift in optimum composition with temperature was attributed to a shift in the rate-determining step from CH_3OH adsorption/dehydrogenation at room temperature to the surface reaction between the dehydrogenated intermediate and surface oxygen at 60°C. Methanol oxidation current densities at 0.4V in 0.5M H_2SO_4 and 0.5M CH_3OH for various temperatures are shown (Fig. 3) for an alloy with the optimum Ru surface composition under these conditions (~30 at%). The apparent activation energy for this surface was measured to be 60 kJ/mole as inferred from an Arrhenius plot of ln(i) *vs* 1/T (Fig. 3, insert). Current densities in terms of current per unit mass of exposed metal for our smooth model catalysts are in good agreement with activities measured on supported high-surface-area electrodes, suggesting that there is no fundamental difference between these two types of catalysts, *i.e.*, that there is no significant particle-size effect or metal-support interaction.

Poisoning of Fuel Cell Electrocatalyst Surfaces: NMR Spectroscopic Studies

Platinum is the most active single-component catalyst for CH_3OH electrooxidation in DMFCs; however, poisoning reactions at the surface render the anode ineffective under target operating conditions. Recently, a number of *in situ*, on-line, and *ex situ* techniques have been utilized to obtain information on the nature of the poisoning intermediate(s) in this system. Significant advances have been made toward this end, although no present technique can yield information on practical (supported, dispersed) electrocatalysts *via in situ* analysis.

Nuclear magnetic resonance (NMR) spectroscopy is a quantitative, non-destructive, bulk method of probing the chemical environment of a specific nucleus and has been used successfully as a tool for identifying and characterizing chemisorbed species in gas-phase catalysis. To achieve high sensitivity, NMR requires large sample sizes, which translates into large surface areas for interfacial studies. NMR is therefore particularly well suited, and indeed limited to, studies of practical catalysts. Our research seeks to extend the application of NMR spectroscopy to obtain information about surface poisoning on graphite-supported Pt and Pt-alloy anodes in H_2SO_4 electrolyte containing CH_3OH.

Because CO has been postulated as the main poisoning adsorbate in the CH_3OH electrooxidation reaction, as suggested by *in situ* IR studies on smooth Pt electrodes, we have conducted preliminary studies on a model system of adsorbed ^{13}CO. We have designed and constructed an electrochemical cell for use inside an NMR probe for the observation of ^{13}C magnetization in a 5-cm bore 63 kG magnet (Fig. 4). The working-electrode material is composed of 20 wt% metal on Vulcan XC-72 supported on a carbon cloth. This cloth is rolled tightly to form a cylindrical

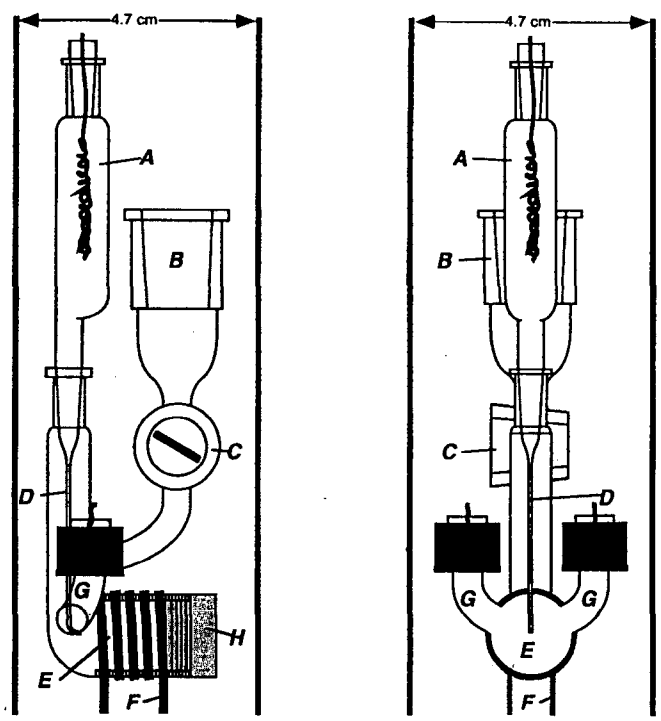

Fig. 4. *Side and rear views of a probe cell used for NMR studies of fuel cell electrocatalyst interfaces. (A) static H_2 reference electrode; (B) electrolyte fill port; (C) stopcock; (D) Luggin capillary; (E) working electrode chamber; (F) NMR coil; (G) sidearms for working electrode lead and counter electrode; (H) PTFE end cap.*

Preliminary experiments have detected the signal from ^{13}CO adsorbed on a 5%Pt/SiO_2 catalyst from the gas phase. We are currently performing experiments to detect and characterize the signal from ^{13}CO adsorbed on the electrodes described above from ^{13}CO-saturated 0.5M aqueous H_2SO_4 under open-circuit cell conditions. With these initial studies we hope to establish the feasibility of NMR for providing *in-situ* information on adsorption at the electrode-electrolyte interface. We will then have a firm base for studying the surface poisoning behavior of the CH_3OH electrooxidation reaction.

References

Adler TC, McLarnon FR, Cairns EJ. Alkaline-Fluoride-Carbonate Electrolyte for Zinc/Nickel Oxide Cells. R&D-100 Award, 1992.

Adler TC, McLarnon FR, Cairns EJ. "Alkaline-fluoride-carbonate electrolytes for enhanced Zn/NiOOH cell cycle-life performance." Paper No. 60 presented at the 184th Electrochemical Society Meeting, New Orleans, LA, October 1993.

Adler TC, Plivelich RF, McLarnon FR, Cairns EJ. Zinc electrodes. In: D.A. Scherson, ed., *Proceedings of the Symposium on the Science of Advanced Batteries.* Cleveland, OH: Case Western Reserve University, 1993.

Dorda AA, McLarnon FR, Cairns EJ. The effect of zinc ions on the platinum electrode in alkaline solutions. *J. Electroanal. Chem.* 1994; 364: 71.

Klein M and McLarnon F. Nickel-zinc batteries. In: D. Linden (ed.), *Handbook of Batteries and Fuel Cells,* 2nd edition. New York: McGraw-Hill Book Company (in press, 1993).

Cairns E, Adler T, McLarnon F. "New electrolytes for rechargeable Zn/NiOOH batteries." Paper presented at the First Annual Conference—Industrial Liaison Program, University of California, Berkeley CA, March 1993.

Striebel KA, McLarnon FR, Cairns EJ. Laboratory-scale evaluation of secondary alkaline zinc batteries for electric vehicles. *J. Power Sources.* 1993; 47:1.

Striebel KA, McLarnon FR, Cairns EJ. "Kinetic studies of oxygen reduction and evolution on metal oxide films produced with pulsed laser deposition." Paper No. 1768 presented at the 183rd Electrochemical Society Meeting, Honolulu, HI, May 1993.

Ridgway PL, McLarnon FR, Cairns EJ. *Performance of Sodium/Phosphorus-Sulfur Cells and Phase Equilibria of Sodium-Phosphorous-Sulfur Mixtures.* Lawrence Berkeley Laboratory Report No. LBL-33082, September 1992.

Cairns EJ, McLarnon FR, Ridgway PL. Sodium-Sulfur-Phosphorus Power Cell. U.S. Patent Assignment, Docket No. IB-910. 1992.

Lessner PM, McLarnon FR, Winnick J, Cairns EJ. The dependence of aqueous sulfur-polysulfide redox potential on electrolyte composition and temperature. *J. Electrochem. Soc.* 1993; 140: 1847.

Rudnicki JD, Brisard GM, Gasteiger HA, Russo RE, McLarnon FR, Cairns EJ. Effect of the supporting electrolyte and beam diameter on probe beam deflection experiments. *J. Electroanal. Chem.* 1993; 362: 55.

Brisard GM, Rudnicki JD, McLarnon FR, Cairns EJ. "Application of the probe beam deflection spectroscopy for the investigation of corrosion behavior of copper in alkaline solutions." Paper No. 1912 presented at the 183rd Electrochemical Society Meeting, Honolulu, HI, May 1993.

Rauhe BR, McLarnon FR, Cairns EJ. *Direct Anodic Oxidation of Methanol on Supported Platinum/Ruthenium Catalyst in Aqueous Cesium Carbonate.* Lawrence Berkeley Laboratory Report No. LBL-32137, July 1992.

Electrode Surface Layers

F.R. McLarnon, R.H. Muller, F.-P. Kong, M. Odziemkowski*

We are using advanced *in situ* and *ex situ* characterization techniques to study the structure, composition and mode of formation of surface layers on electrodes used in rechargeable batteries. The primary objective of this research is to identify film properties that improve the rechargeability, cycle-life performance, specific power, specific energy, stability and energy efficiency of electrochemical cells. Prior work on the evaluation of ion implantation as a means to improve the corrosion resistance of Pb battery electrode current-collector materials has been completed, and our present research seeks to characterize the transformation of surface phases that accompanies the charging and discharging of Ni electrodes in alkaline electrolytes.

Ellipsometric-Electrochemical Study of Oxide Film Formation on Nickel Electrodes

To examine the electrochemical interconversion between $Ni(OH)_2$ (predominant species on a discharged Ni electrode) and NiOOH (predominant species on a charged Ni electrode), and search for an effective way to improve the utilization of active material in porous NiOOH battery electrodes, we have been studying the effects of foreign cations on the electrochemical behavior of solid Ni electrodes. We are especially interested in characterizing the effects of Co additions on the film-forming properties of Ni electrodes, because Co additions are known to increase the charge-storage capacity of porous NiOOH battery electrodes. The exact mechanism by which substituted cations promote or degrade the electrochemical interconversion between $Ni(OH)_2$ and higher-valent Ni oxides is not well understood, and the elucidation of this process is a primary focus of this research effort. Because the electrochemical oxidation of Ni^{2+} species is always accompanied by the unwanted (parasitic) O_2-evolution reaction at the Ni electrode surface, there exists a strong motivation to modify the Ni electrode surface properties. Needed is an appropriate surface treatment that will not only improve the utilization of Ni active material (perhaps by promoting the formation of Ni^{4+} species during the charging process), but also suppress the O_2-evolution reaction.

We have conducted electrode surface-modification experiments using Co, Zr and Pb additions to make the conductivities of both $Ni(OH)_2$ and NiOOH more equal to each other, and to decrease the electrocatalytic activity of the electrode surface for O_2 evolution. These elements were introduced into the surface layers of the Ni electrodes using a newly developed low-energy ion implantation technique known as Metal Plasma Immersion Ion Implantation (MPIII). The MPIII electrode bias potential and the duty cycle of the substrate bias pulser were controlled at -2kV and 50%, respectively, to produce an ion-penetration depth of ~2-3 nm. The dose level of implanted ions was estimated to be ~$2x10^{16}$ atoms/cm^2, and the atomic fraction of foreign atoms at the electrode

*Materials Sciences Division, LBL

surface was estimated to be 30-40%, which is a much higher level than that in electrodes implanted with medium-energy ions. Compared to Co-free Ni electrodes, the electrochemical potentials corresponding to the transformations between $Ni(OH)_2$ and NiOOH during both oxidation and reduction processes shifted to more-negative (reducing) values, and a higher coulombic capacity was obtained. This is the case for the electrodes prepared by using both low- and medium-energy Co implantation. In addition, *in situ* ellipsometric measurements detected a significant amount (up to 30% by volume) of inactive material (probably Co oxide) on the surface of the Co-implanted Ni electrodes.

It has been reported that Zr and Pb may suppress the O_2-evolution reaction, however our initial experiments provided no evidence for such a beneficial effect when these elements were implanted into Ni electrodes. It is possible that passivating Zr or Pb compounds formed on the Ni electrode surfaces and inhibited NiOOH-$Ni(OH)_2$ interconversion. Experiments to further characterize ion-implanted Ni electrodes are underway.

Raman Spectroscopic Studies of the Electrochemical Behavior of Nickel Oxide Electrodes

We have initiated a new Raman spectroscopic study of the surface films that form on Ni electrodes in alkaline electrolytes during charge-discharge cycling. The molecular sensitivity of Raman spectroscopy complements our ellipsometric study of Ni electrode surfaces described above. The goal of our Raman effort is to help determine the mechanism by which additives such as Co alter Ni-electrode film-formation processes and electrochemical properties. For example, if we can identify the chemical states of the Co and Ni species in the films, we can then determine whether Co forms a new surface phase, or instead modifies the properties of the NiOOH/$Ni(OH)_2$ surface layers. We will also seek molecular-spectroscopic evidence for Ni^{4+} species formation, and try to identify means to stabilize this highly oxidized form of Ni.

We will employ three different experimental strategies to characterize film formation on pure and ion-implanted Ni electrodes: 1) Normal *in situ* Raman spectra will be recorded during constant-current charge-discharge cycling, thereby providing data under the same experimental conditions we used for our prior ellipsometric-electrochemical experiments. 2) Surface-enhanced Raman scattering (SERS) experiments will be attempted using a previously established method wherein a small amount of Ag is deposited onto the Ni electrode. In this case, the structure of the deposited Ag will enhance the Raman signal-to-nose ratio, however the presence of Ag may alter the chemical environment at the Ni electrode surface. 3) We will also try to develop a SERS technique in which an acceptable signal-to-noise ratio is obtained without relying upon Ag deposition. In all cases, the experimental regimen will not only replicate those under which ellipsometric data have been previously recorded, but also approximate the conditions in porous NiOOH battery electrodes.

References

Zhang ST, Kong FP, Muller RH. *Effect of Ion Implantation on the Corrosion Behavior of Lead and a Lead-Antimony Alloy*. Lawrence Berkeley Laboratory Report No. LBL-34890. 1993.

Fukunaka Y, McLarnon F, Asaki Z. Laser interferometry as an *in-situ* technique to characterize electrochemical Processes. Chap. 11 in: N. Masuko, T. Osaka and Y. Fukunaka (eds.), *New Trends and Approaches in Electrochemical Technology*. Tokyo: Kodansha Scientific, Ltd. 1993; 215-234.

EXAFS Studies of Electrode Materials for Lithium Batteries

E.J. Cairns, S.P. Cramer, C. Horne

During the last several years, there has been an increasing emphasis on batteries using Li as the negative-electrode active material because of the low electronegativity and equivalent weight of Li, properties amenable for battery systems of high cell voltage and high theoretical specific energy. A key to maximizing the specific energy of Li batteries lies in the positive-electrode active material, wherein high electronegativity, the ability to intercalate Li^+ ions, low equivalent weight, and low cost are desirable properties. Manganese oxides meet these requirements and also possess a relatively low toxicity; however, the low reversibility of Li intercalation for binary oxides of manganese leads to capacity loss with repeated cycling.

The purpose of this research is to obtain a thorough understanding of the Li intercalation process at the atomic level by employing *in situ* x-ray spectroscopic techniques such as Extended X-ray Absorption Fine Structure (EXAFS) and inelastic scattering. Conventional x-ray absorption spectra average the contributions from all species of a given element. The signals from different sites are often unresolved, making interpretation of individual site structures within the spectrum difficult. For oxidation state-specific x-ray absorption, changes in fluorescence energies and intensities will be used to resolve individual oxidation states within the positive electrode's active material by combining high-resolution fluorescence detection with high-resolution absorption measurements. These measurements will take place as the experimental cell is cycled to observe structural and chemical changes as they occur. Precisely tuned, high-intensity x rays generated from synchrotron radiation sources are needed to provide the high sensitivity this research requires. The spectroscopic techniques are expected to yield detailed information about the chemical environment of the Mn atoms as a function of the state of charge or Li content of the positive-electrode active material as well as the number and depth of cycles over which the positive electrode is exercised. Electrochemically characterizing the cell via techniques such as cyclic voltammetry in conjunction with the spectroscopic measurements helps define the structure-property-performance relation.

Planned activities include assembling a spectrograph for use at the Stanford Synchrotron Radiation Laboratory (SSRL), design of appropriate electrochemical cells, fabrication of an electrochemical characterization apparatus, electrochemical characterization of cells, and collection of initial data on the Li-Mn-O system from experiments at SSRL. The LBL Advanced Light Source will be used as a synchrotron radiation source when the appropriate beamline is ready for use.

Application of Pulsed Laser Deposition to the Study of Rechargeable Battery Materials

K.A. Striebel, E.J. Cairns

In this new program, electrocatalytic metal oxide films with perovskite and pyrochlore structures will be prepared by pulsed laser deposition on conductive polycrystalline substrates for mechanistic studies of O_2 reduction and evolution reactions in alkaline battery electrolytes. To illustrate the generality of the technique and to elucidate some fundamental properties critical to the development of secondary lithium batteries, we will also prepare films of the spinel structure for studies of electrolyte stability and Li intercalation reactions.

We have initiated experiments to produce polycrystalline $La_{0.6}Ca_{0.4}CoO_3$ perovskite films on glassy carbon substrates. Films produced to date are less dense than expected due to corrosion of the glassy carbon during the ablation process. Film-covered electrodes have been mounted in the tip of a rotating disk electrode. Preliminary electrochemical measurements and post-test analyses indicate that the perovskite films are quite stable in highly alkaline electrolytes. Voltammetric studies of the $La_{0.6}Ca_{0.4}CoO_3$ films in 30 wt% KOH show at least one redox process occurring in the film at ~0 V *vs.* Hg/HgO, and the films show catalytic activity for the evolution and reduction of O_2. Optimization studies of the ablation process to produce films of other metal oxides and to improve film density are underway.

Fundamental Characterization of Carbon-Based Materials for Electrochemical Systems

K. Kinoshita

Carbon-based materials have many desirable physicochemical properties for electrochemical systems such as batteries, fuel cells, capacitors, etc. They have excellent corrosion resistance in many electrolytes, acceptable electronic conductivity, good thermal conductivity, and they are available in a wide variety of physical structures. Despite these attractive features, and their widespread usage, there still exists a lack of full understanding of how to control and modify the physicochemical properties of carbon-based materials by chemical or thermal treatments. A fundamental research program on the synthesis, characterization and modification of carbon-based materials to improve their properties for use in electrochemical systems was initiated in FY 1993 under the sponsorship of DOE Basic Energy Sciences' Advanced Battery Technology Research and Development Program. The wetting by aqueous electrolytes, polymer/plastic and carbon interactions, and changes to these properties by modifying the physicochemical properties of carbon-based materials, will be investigated.

Applied Research on Lithium/Polymer-Electrolyte Cells

E.J. Cairns, M. Doeff, T. Fuller*, R. Jiang*, L. Johnson*, L, Kepley*, F. Kong, K. Kinoshita, Y. Lee, F.R. McLarnon, J.S. Newman*, B. Novak* ,T. Richardson*, P.N. Ross*, K.A. Striebel*

LBL and the U.S. Advanced Battery Consortium have entered into a Cooperative Research and Development Agreement (CRADA) to develop advanced Li/polymer-electrolyte battery technology. Investigators from both the Energy and Environment Division and the Materials Sciences Division are participating in this effort. Research tasks include the study of electrochemical phenomena at electrode/polymer electrolyte interfaces, the development of advanced mathematical models of Li/polymer-electrolyte cells, the synthesis of improved polymer electrolytes and materials for positive electrodes, the establishment of an extensive biblio-graphic database on components for Li/polymer-electrolyte cells, and an investigation of overcharge/overdischarge phenomena in secondary Li cells.

*Materials Sciences Division, LBL

Chemical Applications

High-Temperature H_2S-Removal and Sulfur-Recovery Processes

L.A. Fenouil, S. Lynn

This project explores the technical and economic feasibility of a high-temperature process for cleaning coal gas prior to combustion in a gas turbine used for power production. In the process the coal gas would pass through a nearly isothermal, moving bed of freshly calcined calcium carbonate that would serve to remove particulates (by filtration), hydrogen sulfide (by chemisorption), and ammonia (by catalysis). The objective of this research is to define the temperature range within which these goals can best be realized at a given pressure. Preliminary calculations indicate a probable range 850 to 1000°C, close to the outlet temperature of most gasifiers.

Sorption of H_2S With Calcined Limestone

The process under investigation involves removal of H_2S from the coal gas by sorption into a countercurrent moving bed of limestone particles. Ammonia in the coal gas will be broken down by catalysis, and gasifier fines will be removed by cycloning and by filtration by the moving granular bed. This project is focusing on developing the necessary description of the kinetics of the reactions of H_2S with lime and limestone, and in particular the evolution of the structure of the solids during the course of these reactions using a differential quartz tube reactor. Because studies at gasification pressures would require very much more expensive apparatus, this study is confined to atmospheric pressure.

The main reaction of importance in the limestone/H_2S system is:

$$CaCO_3 + H_2S \leftrightarrow CaS + H_2O + CO_2 \quad (1)$$

which is favorable at temperatures above 704 K. The external dimensions of the solid are observed to remain constant, suggesting that the porosity of the solid increases with conversion, which would lead to a fast reaction and high conversion. At high temperatures, limestone also undergoes calcination if the fugacity of CO_2 is low enough:

$$CaCO_3 + H_2S \leftrightarrow CaO + CO_2 \quad (2)$$

The lime formed can then react with H_2S via:

$$CaO + H_2S \leftrightarrow CaS + H_2O \quad (3)$$

The composition of the gas phase is dictated by the initial C:H:O ratio and the equilibrium of the water gas shift reaction as a function of temperature:

$$CO + H_2O \leftrightarrow CO_2 + H_2 \quad (4)$$

Failure to account for calcination and water-gas-shift equilibration has cast doubt on the validity of most previous studies in this system, therefore a fresh evaluation of the kinetics is being made.

Calcium carbonate. Initial experiments with limestone sulfidation indicated a significant drop in the rate of sorption of H_2S after only 10 to 15% conversion of the $CaCO_3$ to CaS. Examination of the sulfided particles by microscopy showed them to be much smoother than the original limestone, indicating that some sort of sintering was occurring. When reagent-grade CaS powder (average grain size about 1.7 μm) is heated under an atmosphere of 96% CO_2–4% H_2, the CaS loses about 25% of its initial BET surface area (1.2 to 1.3 m^2/g) in 80 minutes at 1033 K, more than 50% in the same time at 1181 K.

Calcium oxide. In contrast to the case of the reaction between $CaCO_3$ and H_2S, the reaction rate between CaO and H_2S is rapid enough to allow complete conversion of CaO to CaS in about 1 to 2 hours for lime particles of 1 millimeter in diameter exposed to simulated coal gas containing about 1% H_2S. For example, limestone particles were calcined at 915°C for varying lengths of time in an atmosphere of CO_2: 88%; CO and H_2O: 4.75%; H_2: 0.8%; H_2S: 1.7% The results are shown (Fig. 1). Note that prolonged heating at 915°C prior to sulfidation has relatively little effect on the rate of CaO and H_2S uptake once sulfidation is begun. A log-log plot of the data from Fig. 1 yields a slope of 0.5 to 0.6, which is characteristic of a rate controlled by diffusion through the product layer (here, CaS).

At 915°C, in an atmosphere containing 88% CO_2, the intrinsic limestone calcination rate, from $CaCO^3$ to CaO, is

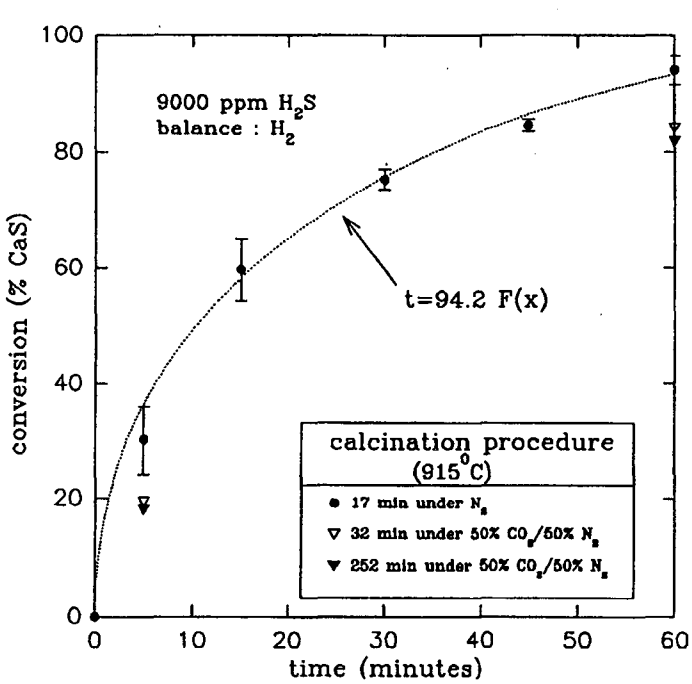

Fig. 1. *Conversion of CaO to CaS as a function of time for a single-pellet reactor. (F(X) is defined in the text).*

slower than that of lime sulfidation, from CaO to CaS. The overall conversion of $CaCO_3$ to CaS is then limited by the rate of lime formation and not by that of lime sulfidation. At 945°C (which corresponds to about 50°C above the limestone calcination temperature for a gas containing 88% CO_2) the rate of limestone calcination is faster than the sulfidation rate, so that the actual chemical reaction is between Ca) and H_2S, not between $CaCO_3$ and H_2S. Precalcining the limestone then has very little effect on the overall conversion of the stones to CaS. Data were also obtained at 1015°C, and there was only a weak effect of temperature on the sulfidation rate. CaO sintering, much more significant at 1015°C than at 945°C, thus appears to have little effect on the reaction kinetics of sulfidation.

Calcined limestone was exposed to very low levels of H_2S to determine whether there was a change in the apparent reaction kinetics as the level of H_2S was reduced to near that desired in a cleanup process. The results show that at 915°C the reaction is still diffusion-controlled at an H_2S level of about 500 ppm. It also seems that the reaction rate is still proportional to the difference between the H_2S concentration in the gas phase and its equilibrium concentration in the presence of CaO, in accordance with the kinetic model developed in the following section.

Kinetic data. To gather detailed and precise kinetic data for design purposes, we changed our experimental procedure from a "mini-bed" reactor to a single-pellet differential reactor. The gas flow was increased to its largest possible value to prevent any significant gas-phase mass-transfer resistance. The data obtained using a reactor gas containing 9000 or 900 ppm of H_2S in H_2 and N_2 are shown in Fig. 2. SEM pictures and sulfur maps (EDAX) on the reacted limestone particles show the steady buildup of a layer of CaS. Thus, the experimental data were fit to a shrinking-core model for spherical particles, using the following kinetic equation:

$$t = \tau_1 [1 - 3 (1-X)^{2/3} + 2 (1-X)] = \tau_1 F(X) \quad (5)$$

with

$$\tau_1 = \frac{\rho_s R^2}{6(C - C_{eq}) D_e} \quad (6)$$

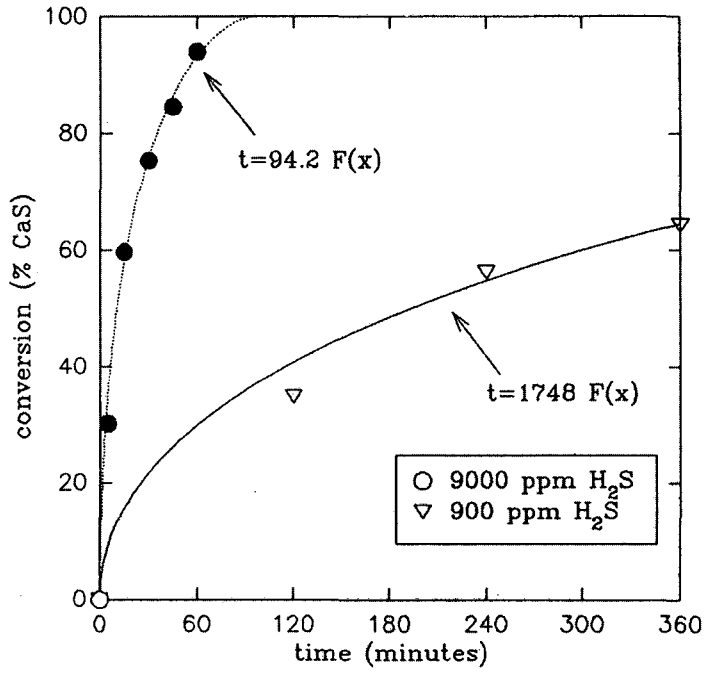

Fig. 2. *Conversion of CaO to CaS as a function of time for a single-pellet reactor. (F(X) is defined in the text).*

where:
t = time (s)
X = conversion of the solid reactant
ρ_s = molar density of the reacting solid (mol/m³)
C = concentration of H_2S in the gas phase (mol/m³)
C_{eq} = equilibrium concentration of HS under experimental conditions (mol/m³)
D_e = effective diffusivity of H_2S in the sulfide layer (m²/s)
R = pellet radius (m)

Bed modeling for a moving bed of sorbent using the shrinking-core model. Using the kinetic data above, it is possible to model the performance of a moving bed of lime or limestone with the help of some simplifying assumptions.

Assumptions

- isothermal bed;
- steady-state, N and u_G are constant;
- plug-flow conditions for the gas phase and the solid phase with no axial dispersion, *i.e.*, one-dimensional model along the z-axis (no radial variation);
- ε is constant along the bed;
- the shrinking-core model for spherical particles describes the sulfidation kinetics at the particle level;
- the solid particles all have the same diameter;
- the gas is ideal.

Results

The equations that result from these assumptions can be combined and solved analytically to give:

$$Z = \left(\frac{Sh' - 1}{Sh'}\right) F(Y) + 3 Y_{eq}^{-1/3} G(Y) \quad (7)$$

where

$$F(Y) = \ln\left[\frac{(A^3-1)A_{in}^3}{(A_{in}^3-1)A^3}\right] \tag{8}$$

and

$$G(Y) = -\frac{1}{6}\ln\left[\frac{(1-A)^3(1-A_{in}^3)}{(1-A^3)(1-A_{in})^3}\right] + \frac{1}{\sqrt{3}}\left[\tan^{-1}\left(\frac{2A+1}{\sqrt{3}}\right) - \tan^{-1}\left(\frac{2A_{in}+1}{\sqrt{3}}\right)\right] \tag{9}$$

$$A = \left(\frac{Y_{eq}}{Y}\right)^{1/3} \tag{10}$$

$$A_{in} = \left(\frac{Y_{eq}}{Y}\right)^{1/3} \tag{11}$$

The length of the bed (and the H_2S profile) is a function of four parameters: Sh′, Pe′, y_{eq} and R. It is interesting to note that for a given Sh′ and y_{eq} (which is fixed by the thermodynamics of the limestone sulfidation reaction), the bed length is proportional to the product R × Pe′.

X_{in} and C_{in} (or y_{in}) are fixed by the process conditions, *i.e.*, by the concentration of H_2S of the coal-gas to be treated and by the degree of conversion of the sorbent entering the bed. We are free to chose X_{out} (which will determine the degree of sorbent utilization) and y_{out} (which will determine the degree of H_2S removal from the coal gas), provided that y_{out} is larger than y_{eq}. The maximum value of the superficial velocity u_g is the fluidization velocity of the bed if the gas is flowing vertically in the upward direction. The solid flow rate is then fixed by the overall mass balance. Equation 7 can be used to obtain the H_2S profile within the moving bed; the total bed length is obtained by inserting Y_{out} for Y in Eq. 7.

Figure 3 shows an example of calculations using reasonable values of the various physical parameters of the CaO/H_2S in coal-gas system. The Sherwood number is used as a free parameter to demonstrate the influence that external mass-transfer can have on the system. It can be seen that the required length of the $CaCO_3$ bed will be somewhere between a few centimeters and one to two meters. The required bed length is always larger if the gas and solid flow concurrently than for the countercurrent configuration because the reaction rate decreases with decreasing H_2S concentration and increasing CaS conversion.

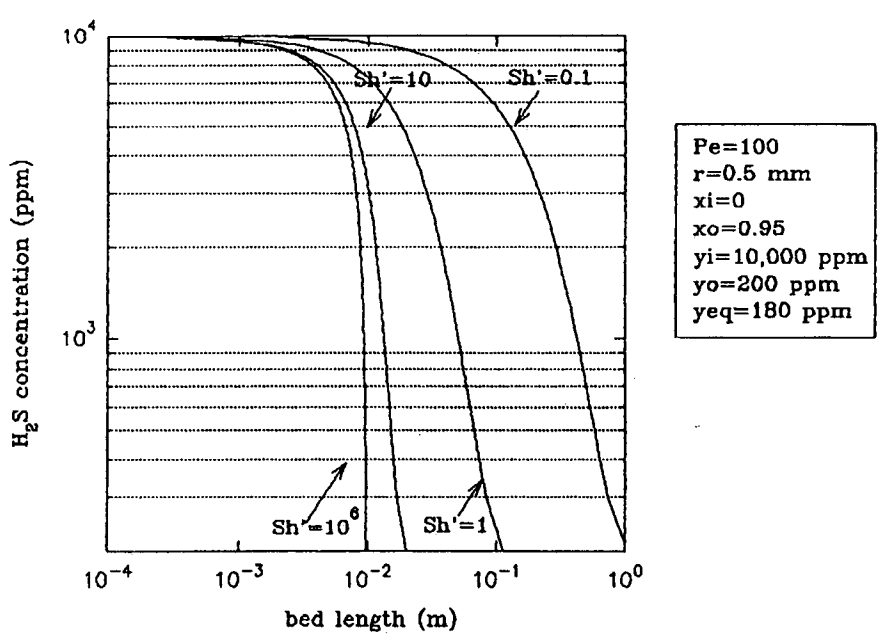

Fig. 3. *H_2S concentration as function of the bed length for countercurrent flow configuration.*

Separations by Reversible Chemical Complexation

C.J. King, L.A. Tung, R. R. Broekhuis, J.H. Lee, S. Lynn

Carboxylic acids, glycols and related substances are among the most attractive products that can be manufactured from biological raw materials by fermentation. Recovery of these products from fermentation media is difficult, because the solutions are dilute and complex. Separations of these substances from dilute aqueous solutions are also important for petrochemical manufacture of several large-volume chemicals, such as acetic acid and ethylene and propylene glycols, and for processing of waste streams. Separations involving reversible chemical complexation have strong potential for processing of these streams, and are the focus of our research.

Recovery of Glycols by Reversible Complexation or Reaction

The recovery of glycols from aqueous solutions is greatly complicated by the facts that they are highly hydrophilic, do not crystallize and are less volatile than water. We have studied and evaluated a recovery method based upon reversible reaction of glycols with aldehydes to form dioxolanes (cyclic acetals). By virtue of their low polarities, dioxolanes are much more volatile and readily extractable than are the glycols themselves. The recovered dioxolane is converted back to product glycol and aldehyde, either directly by hydrolysis or indirectly through methanolysis. In these reactions it is important to devise effective means of forcing the equilibria in the desired directions, such as by carrying out the reactions in distillation columns with high hold-up and appropriately placed feeds.

We measured equilibria and kinetics for formation of dioxolanes by reactions of formaldehyde and acetaldehyde with 1,2-propanediol. We also measured vapor-liquid and liquid-liquid equilibria in these systems. Rates are somewhat slow, but are accelerated with sufficient amounts of catalysts, which can be acidic polymeric resins.

The solution chemistry of formaldehyde considerably reduces its volatility over aqueous solution. Hence it is difficult to remove excess formaldehyde in the case of reaction of 1,2-propanediol with formaldehyde to form 4-methyldioxolane, yet excess formaldehyde is needed to produce a sufficient concentration of the dioxolane.

The rate of reaction of propylene glycol with acetaldehyde is substantially greater than that with formaldehyde, again because the solution chemistry of formaldehyde suppresses the kinetics. However acetaldehyde itself distributes substantially to the vapor phase in a distillation or stripping process, thereby reducing the concentration of acetaldehyde in the liquid phase and thus the equilibrium conversion to the dioxolane, in this case 2,4-dimethyldioxolane. We therefore investigated a fully liquid-phase reaction, with the product dioxolane being extracted into an appropriate solvent. Extraction with an alkyl aromatic, such as ethylbenzene or xylene, is effective. The full process for reversible extractive reaction of 1,2-propanediol to form 2,4-dimethyldioxolane involves several sequential steps, but should be substantially less energy intensive than simple distillation of a glycol-water feed.

We are also continuing our earlier research on the recovery of glycols and sugars from aqueous solution by reversible complexation with organoboronates. We are currently seeking the most suitable boronate extractant or sorbent and are considering methods of regeneration.

Recovery of Carboxylic Acids at $pH > pK_a$

We have demonstrated that solid sorbents with pendant amine groups can maintain capacity for uptake of carboxylic acids from aqueous solutions at values of pH two or more units above the pK_a of the carboxylic acid. This is important because fermentations to produce most acids work effectively only under such conditions. Amine-based extractants also have this capability if they are mixed with a diluent, such as octanol, that effectively solvates the acid-amine complex. Through measurements and interpretation of equilibria, we have shown that these results can be interpreted quantitatively through formation of 1:1 and 1:2 amine:acid complexes, along with tendencies for incorporation of additional carboxylic acid molecules into the complex.

Regeneration of these sorbents and extractants can be accomplished by back-extraction with aqueous trimethylamine (TMA), followed by thermal decomposition of the trimethylammonium carboxylate to form recycle TMA vapor and product acid. Carboxylic acids with sufficiently low solubility precipitate, while very soluble acids, such as lactic acid, can be recovered by conversion of the trimethylammonium carboxylate to an ester, followed by distillation of the ester.

We have also investigated competitive uptakes of sulfate, phosphate and carboxylate anions by amine-based sorbents and extractants. The competition from the inorganic anions is substantially less for the extractants, presumably because the organic environment accommodates the carboxylate better than it does sulfate or phosphate.

We are currently seeking other methods of regenerating the basic sorbents and extractants that are effective for taking up carboxylic acids at $pH > pK_a$.

Separations Based upon Water-Enhanced Solvation

In earlier research, we demonstrated that solubilities of dicarboxylic acids in certain electron-donor solvents are greatly increased by the simultaneous presence of relatively small amounts of water. This led to a simple method for recovery of sparingly soluble carboxylic acids (*e. g.*, adipic, fumaric) by extraction with a ketone, such as methyl cyclohexanone, followed by selective stripping of the co-extracted water, causing the acid to precipitate. The phenomenon results from a substantial increase in the activity coefficients of these solutes in electron-donor solvents. Other applications of the phenomenon of water-enhanced solvation could be important. For example, leaching of carboxylic acids from solid sorbents with electron-donor solvents would be enhanced by the presence of water in the solvent.

We used two experimental methods, vapor-headspace gas chromatography and solubility measurements, to determine the effects of water on the activity coefficients of several different carboxylic acids, ethanol, 1,2-propanediol, and several phenols in ketone and ester solvents. These solutes were picked by screening literature data for related phenomena. In cyclic ketones and *n*-butyl acetate, solute activity coefficients decreased by factors of 2 to 3, 6 to 8, and 7 to 10 due to the presence of water for mono, di- and tri-carboxylic acids,

respectively. Activity coefficients of ethanol and 1,2-propanediol decreased by factors of about 1.5 due to co-dissolved water. Water enhancement of the solvation of phenols was small, when existent.

For carboxylic acids, the phenomenon of water-enhanced solvation is large enough to serve as the basis for attractive separation processes. For alcohols, diols and phenols the degree of water enhancement appears not to be sufficient for that purpose.

References

King CJ. Solvent extraction in the process industries: quo vadis? In: *Proceedings, ISEC'93: The International Solvent Extraction Conferencee*. London: Society of Chemical Industry 1993; 1: 3-14.

Lee JH, King CJ. *Water-Enhanced Solvation of Organics*. Lawrence Berkeley Laboratory Report No. LBL-34410, July 1993.

Randel LA, Chow, TK. Ion-pair extraction of multi-OH compounds by complexation with organoboronate. *Solvent Extr. & Ion Exch* (in press, 1993).

Tung LA, King CJ. Regenerable extraction and sorption of carboxylic acids from aqueous solutions at pH > pK_a. In: *Proceedings, ISEC'93: The International Solvent Extraction Conference*. London: Society of Chemical Industry, 1993; 2: 1010-1017.

Tung LA, King, CJ. *Recovery of Carboxylic Acids at pH Greater than pK_a*. Lawrence Berkeley Laboratory Report No. LBL-34669, August 1993.

X-Ray Absorption Spectroscopy of Metalloproteins and Related Systems

S.P. Cramer, J. van Elp, X. Wang, J. Moore

We have developed two new types of x-ray spectroscopy to study the atomic and electronic structures of metal clusters in metalloproteins, as well as the spin states and spin coupling in these clusters. Experiments were performed at the National Synchrotron Light Source (NSLS at BNL) and the Stanford Synchrotron Radiation Laboratory (SSRL at SLAC). Both new techniques: High Resolution Fluorescence Spectroscopy and X-Ray Magnetic Circular Dichroism, will benefit from high brightness, high flux, and circular polarized light offered by Advanced Light Source (ALS).

High-Resolution Fluorescence Spectroscopy

Site-specific x-ray absorption is based on small shifts in fluorescence energies that occur with oxidation state changes. Thus it is sensitive to specific oxidation states, spin states and site symmetries. The site- and chemical state-selectivity of this technique makes it a powerful tool for probing the structures of mixed-valence compounds and multi-metal clusters in metalloproteins. We have built an x-ray spectrograph and demonstrated fluorescence shifts for Mn(II), Mn(III), and Mn(IV). Because of the difference in exchange coupling, the emitted fluorescence energies due to spin-up and spin-down electrons are different. One can select the spin states by monitoring the different fluorescence peaks. Measured spin-selected XANES spectra of the Mn(II) compound are shown (Fig. 1). These results show that High Resolution Fluorescence Spectroscopy is a useful method to distinguish specific sites of a particular element in a cluster and to study its special properties, such as the spin-resolved local density of states and local magnetic environment of the selected site.

X -Ray Magnetic Circular Dichroism (XMCD)

In an XMCD experiment, the absorption of left- and right-circular polarized light by a magnetized sample is compared. We have studied a mixed-valence Fe(II)/Fe(III) paramagnetic complex using XMCD. The spectra reveal that the coupling between two Fe atoms is antiparallel at 1T, and becomes parallel at 6T (Fig. 2). This is consistent with the ~2.5 wavenumber^{-1} coupling constant of the system. The study shows that XMCD can interpret the coupling pattern in mixed-valence and mixed-metal spin-coupled clusters, and allow one to determine the magnetic orientation of a specific metal in different oxidation states. This technique should have broad applications to bioinorganic chemistry.

Fig. 1. *Spin-selected spectra of Mn(II) compound. Spin-down (top), spin-up (middle), normal transmission spectrum (bottom).*

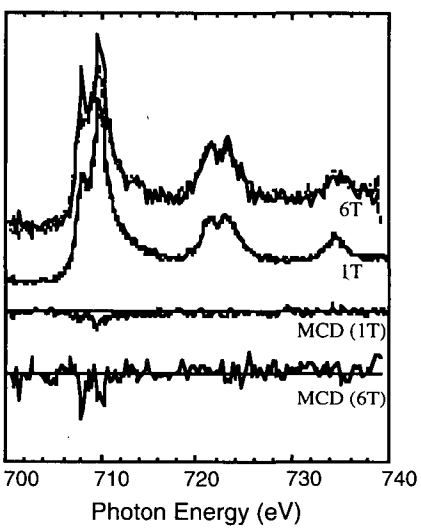

Fig. 2. *XMCD spectra of mixed-valence Fe dimer measured at 1 and 6 Tesla.*

References

Chen J, Christiansen J, Campobasso N, Bolin JT, Tittsworth RC, Hales BJ, Rehr JJ, Cramer SP. Refinement of a model for the nitrogenase Mo-Fe cluster using single crystal Mo and Fe EXAFS. *Angewandte Chemie* 1993.

Chen J, Christiansen J, George S, Tittsworth R, Hales B, Campobasso N, Bolin J, Cramer SP. X-ray absorption spectroscopy of nitrogenase Mo-Fe protein. In: Perry D, Shinn N, Stockbauer R, D'Amico K, Terminello L, eds.. *Applications of Synchrotron Radiation Techniques*

to Materials Science. San Francisco, 1993: 63-68.

van Elp J, Peng G, Seale BG, Mitra-Kirtley S, Huang YH, Johnson MK, Zhou ZH, Adams MWW, Maroney MJ, Cramer SP. Electronic structure and symmetry in nickel L-edge x-ray absorption spectroscopy, application to a nickel protein. *J. Am. Chem. Soc.* (in press).

Peng G, deGroot FMF, Hämäläinen K, Moore JA, Wang X. High-resolution manganese x-ray fluorescence spectroscopy—oxidation state and spin state sensitivity. *J. Am. Chem. Soc.* (in press)

Mullins OC, Mitra-Kirtley S, van Elp J, Cramer SP. Molecular structure of nitrogen in coal from XANES spectroscopy. *Appl. Spectr.* 1993; 47: 1268.

Mitra-Kirtley S, Mullins OC, Branthaver JF, Cramer SP. Nitrogen chemistry of kerogens and bitumens from x-ray absorption near-edge structure spectroscopy. *Energy & Fuels* 1993; 7: 1128.

George GN, Cramer SP, Frey TG, Prince RC. X-ray absorption spectroscopy of oriented cytochrome oxidase. *Biochem. Biophys. Acta* 1993; 1142: 240.

Chen J, Christiansen J, Tittsworth R, Hales B, George SJ, Coucouvanis D, Cramer SP. Iron EXAFS of *A. vinelandii* nitrogenase Mo-Fe and V-Fe proteins. *J. Am. Chem. Soc.* 1993; 115: 5504.

Chen J, Christiansen J, George S, van Elp J, Tittsworth R, Hales B, Alahmad S, Coucouvanis D, Campobasso N, Bolin J, Cramer SP. EXAFS and L-edge spectroscopy of nitrogenase FeMo protein. In: Stiefel E, Coucouvanis D, Newton W, eds. *Molybdenum Enzymes, Cofactors, and Model Systems.* Washington, D.C.: American Chemical Society, 1993: 231-242.

van Elp J, George SJ, Chen J, Peng G, Chen CT, Tjeng LH, Meigs G, Lin HJ, Zhou ZH, Adams MWW, Searle BG, Cramer SP. Soft x-ray magnetic circular dichroism—a new probe for studying paramagnetic bioinorganic systems. *Proc. Natl. Acad. Sci. U.S.A.* 1993; 90: 9664.

George SJ, Lowery MD, Solomon EI, Cramer SP. Copper L-edge spectral studies—a direct experimental probe of the ground-state covalency in the blue copper site in plastocyanin. *J. Am. Chem. Soc.* 1993; 115: 2968.

Mitra-Kirtley S, Mullins OC, van Elp J, Cramer SP. Nitrogen chemical structure in petroleum asphaltene and coal by x-ray absorption spectroscopy. *Fuel* 1993; 72: 133.

Mitra-Kirtley S, Mullins OC, van Elp J, George S, Chen J, Cramer SP. Determination of the nitrogen chemical structures in petroleum asphaltenes using x-ray absorption spectroscopy. *J. Am. Chem. Soc.* 1993; 115: 252.

Fundamental Studies of Laser-Material Interactions

R.E. Russo, M.A. Shannon, X.L. Mao, W.T. Chan

With the advent of processes such as laser-sampling for chemical analysis, pulsed-laser annealing, and pulsed-laser deposition of thin-films, there is a growing need to understand laser-energy coupling to a solid in real time.. However, monitoring changes during laser-material interactions can be quite difficult. For example, detecting a solid-to-liquid phase transition by changes in reflectivity for a material such as aluminum, which undergoes small changes in reflectivity (< 10%) at melt, is difficult. Similarly, detecting melt by measuring temperature changes at a surface can be challenging if the transients are fast (< 1 ms), and if the spatial resolution is small (< 1 mm). Our work fundamentally investigates the nature of laser-material interactions. Several complementary experimental techniques are used to investigate the interactions, including monitoring optical emission for the ablation plume, measuring crater profiles versus gas composition and pressure, detecting acoustic waves in the target, plus other methods. This report describes only the work to directly monitor the solid-to-liquid phase change in real time.

In this work, the onset of melt at the surface of a solid has been detected in real time using a transient photothermal deflection (PTD) technique. PTD is attractive for monitoring events in real time due to

- the ability to detect fast transients (t <20 ns);
- high sensitivity to small changes in flux;
- high spatial resolution (< 10 mm).

Also, unlike direct methods for measuring reflectivity, emissivity or temperature, PTD gives a measure of gradients because a gradient in the index of refraction of the medium deflects light that passes through it. Because temperature gradients ∇T are directly related to heat flux q by a coefficient $k(T)$, through Fourier's law ($q = k \nabla T$), PTD can be exploited to directly measure heat-flux leaving a surface. In practice, the temporal PTD signal can be quite complex due to variations in thermal and optical properties, evolution of vapor, chemical oxidation, geometry, etc. (Fig. 1), making it difficult to discern the physical processes occurring.

Phase transition at the surface of a laser-heated target is detected by the presence of a local maximum and mini-

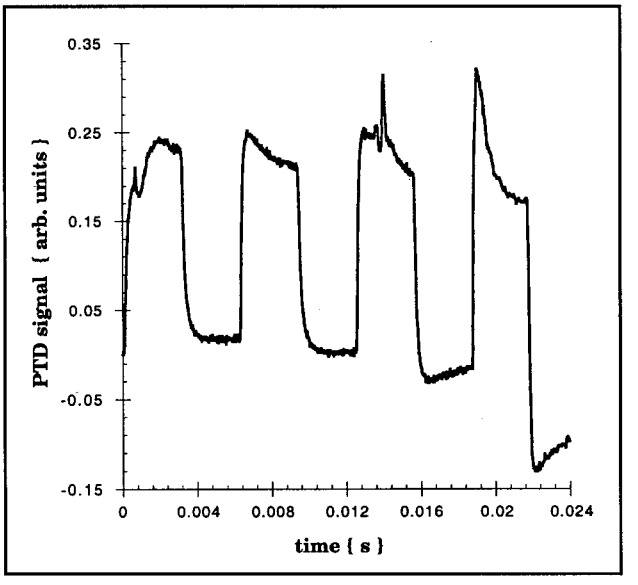

Fig. 1. *Multiple heating cycles show different PTD responses. Coated indium target undergoes melt, oxidation, and laser drilling with an average incident fluence of 2.50 (10^4) W/cm^2. z_o is approximately 100 μm.*

mum pair in the deflection response of a probe-beam passing near the surface. The temporal PTD response of the first heating cycle for an indium target is shown (Fig. 2). The important observation for detecting the onset of melt with PTD is that the first local maximum/minimum pairs found in Fig. 2 occurs only with phase change, and not with simple heating. Also, our analysis shows that this response can not occur if a planar heating source is used. However, when a small laser heating source is used, a local maximum/minimum pair in the PTD can occur at the onset of melt.

The main parameters governing the detection of phase change at the target surface are the sensible heat and the latent heat of melting, as well as the thermal diffusivity of the target and the deflecting medium. For a process wherein the latent heat is larger than the sensible heat, a probe beam can deflect toward the target, causing a local minimum to occur in the temporal PTD response. By modifying the deflecting medium, the ratio of the thermal diffusivities can be changed separately from the ratio of the sensible heat to the latent heat, which can enhance or suppress the minimum. An important finding of this work is that the effect of latent heat of melting can be directly observed at a surface. When the thermal diffusivities are equal and there is no phase change, no maximum or minimum can be observed. However, with phase change, a local minimum can occur in the PTD signal. Moreover, the relative depth of the minimum to the first local maximum will increase as the latent heat of melting grows larger with respect to the sensible heat. The class of materials for which this technique will work is, from a practical standpoint, restricted to materials wherein the latent heat of melting is larger than the sensible heat as determined by its melting temperature and the ambient temperature, and where its thermal diffusivity at melt is similar to or smaller than that of the deflecting medium. An example of an important material that meets these criteria is silicon in an argon atmosphere initiallyat room temperature.

References

Shannon MA, Rostami AA, Russo RE. Photothermal deflection measurements for monitoring heat transfer during modulated heating of solids. *J. Appl. Phys.* 1992; 71 (1): 53.

Shannon MA, Rubinsky B, Russo RE. Detecting laser-induced phase change at the surface of solids via latent heat of melting with a photothermal deflection technique. (Accepted by *J. Appl. Phys.* November 1993).

Mao XL, Chan WT, Shannon MA, Russo RE. Plasma shielding during picosecond laser sampling of solid materials by ablation in He versus Ar atmosphere. *J. Appl. Phys.* 1993; 74 (8):4915.

Shannon MA. Laser-material interactions: a study of laser energy coupling with solids. Ph.D. thesis, University of California at Berkeley, 1993.

Xu X, Russo RE, Grigoropoulos CP. Heat transfer in excimer melting of thin polysilicon layers. (Submitted to *J. Heat and Mass Transfer*, October 1993).

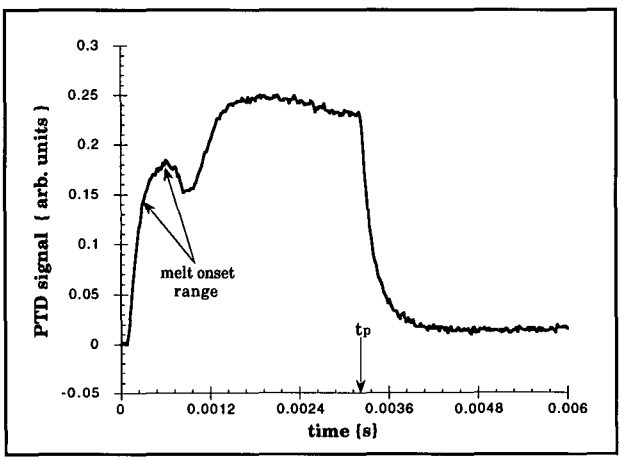

Figure 2. *PTD response for indium target that shows a local maximum and minimum pair after melt begins, followed by another maximum and decline. Average incident fluences is 2.25 (10^4) W/cm^2, and z_o is approximately 100 μm.*

Photothermal Deflection Spectroscopy Of Uranium Oxidation and Dissolution

R.E.Russo, J.D. Rudnicki

Photothermal Deflection Spectroscopy (PDS) is being used to study the dissolution chemistry of uranium dioxide. Knowledge of the dissolution mechanism is needed to develop storage sites for spent fuel. Samples of uranium oxide, which are depleted of uranium-235, are used as surrogates for spent fuel. It is assumed that release of nonvolatile radioisotopes will be mostly governed by the dissolution of the uranium oxide matrix. Studies are being performed in pH 9-10, 0.5 M Na_2SO_4 electrolytes. The PDS technique measures the concentration gradients formed near the uranium oxide surface and the optical absorption of the surface. Both of these measurements are performed *in situ* under dynamic conditions. Electrochemical techniques are used to control the redox conditions of the uranium dioxide sample.

The experiments we perform are windowed cyclic voltammetry experiments. In these experiments, the electrode potential is swept starting from a reducing potential to an oxidizing potential and then swept back to a reducing potential. The oxidizing potential is increased on each successive sweep. The concentration gradients have shown that dissolution from the uranium oxide begins at potential of about -200 mV (*vs.* standard calomel electrode), a potential lower than previously reported in the literature. Sustained dissolution occurs from the uranium dioxide sample after an oxidizing potential of +300 mV has been applied. This dissolution continues even after the sample is returned to reducing potentials. The dissolution rate increases when the electrode is raised to +300 mV a second time. Because the dissolution continues at reducing potentials, the mechanism must be nonelectrochemical. The increase in the dissolution rate after the second sweep to +300 mV is not consistent with the formation of a homogeneous film. Instead, we suggest the dissolution is occurring from specific sites on the sample surface. Each sweep to 300 mV forms additional sites.

A significant change in the optical absorption of the surface accom-

panies the sustained dissolution behavior. The optical absorption changes again when the electrode is raised to +300 mV a second time. The magnitude of these changes is too large to be explained by the formation of a thin film of higher oxide on the uranium dioxide substrate. The optical data also suggest that specific sites on the surface are being converted.

The concentration gradient and optical results are consistent with mechanisms discussed in literature. Once the uranium stoichiometry reaches a critical hyperstoichiometry, surface recrystallization occurs from the face-centered cubic to orthorhombic structure. The recrystallization is accompanied by dissolution of uranyl. Our data suggest that once the crystallization is started at seed sites on the surface, it continues into the surrounding material regardless of the redox conditions. Each sweep to +300 mV forms additional recrystallization seeds.

References

Rudnicki JD, Russo RE. Photothermal deflection spectroscopy investigations of uranium dioxide oxidation. *Materials Research Society Symposium: Scientific Basic for Nuclear Waste Management*, 1992; 294: 55.

Russo RE, Rudnicki JD. Investigations of uranium electrochemistry using photothermal deflection spectroscopy. In: *Proceedings of the International High Level Radioactive Waste Management Conference*, Las Vegas, NV, April 1993.

Rudnicki JD, Shoesmith DW, Russo RE. Photothermal deflection spectroscopy investigations of uranium dioxide oxidation. (submitted to *J. Electroanal. Chem. and Interfacial Chem.*, June 1993).

Sensors for Remote Monitoring

*R.E. Russo, G.L. Klunder, R.J. Silva**

The increasing need to monitor contaminated groundwater has placed a large emphasis on the development of instruments for remote, *in situ* characterization. Onsite or *in situ* chemical analysis can provide rapid screening of samples while minimizing worker exposure. Absorption spectroscopy is one of the most reliable techniques available for the qualitative and quantitative determination of sample composition. With the advances in fiberoptic technology, using light for remote *in situ* sensing of groundwater contaminants has become practical.

Porphyrin dyes are highly sensitive indicators for the spectrophotometric determination of metal ions. An optochemical sensor for the detection of heavy metals has been developed in which a porphyrin dye is immobilized in a cation exchange membrane. The measured absorbance through the membrane is proportional to the metal concentration and the time that the sensor resides in the solution. Limits of detection with this sensor are $5*10^{-8}$ M (6 ppb) Cd^{2+} and $2*10^{-7}$M (40 ppb) Hg^{2+}; other ions such as Zn^{2+} and Cu^{2+} have been quantitatively detected. Metalions studied in this laboratory have radii which allow them to be incorporated into the porphyrin binding cavity, which is approximately 2.0 Å. Based on ionic radii, the lanthanide and actinide ions should be able to incorporate into the porphyrin cavity.

A long pathlength fiberoptic evanescent field absorption sensor was developed to increase the pathlength (increase the light/analyte interaction) and therefore should lead to lower limits of detection. As light propagates down the length of an optical fiber, standing waves are created at each reflection of the core/cladding interface. A portion of the light, known as the evanescent field (or wave), penetrates into the cladding material, where it can be absorbed by the anolyte. The penetration depth is typically on the order of the wavelength and the number of reflections in the fiber can be adjusted by changing the fiber sensor length or the fiber diameter. In this study, the cladding material was replaced with an ion-exchange membrane containing an immobilized dye. The minimum length of a 400-μm core fiber required to obtain an equivalent pathlength to the 3-5 μm thickness of a Nafion membrane is approximately 10 cm. The protective nylon jacket and the polysiloxane cladding materials of the fused silica fibers were removed. The bare quartz fiber was then dipped into the Nafion solution and allowed to air dry. The thickness of the dip coated Nafion was not measured, but is estimated to be 6-10 μm based on other dip coating results. Unfortunately, the Nafion membrane offers little or no protection for the glass fiber which was found to be too fragile and spectra could not be obtained.

Determination of complexation of the metal ions of interest with meso-tetra(n-methyl-4-pyridyl) porphyrin (TMPyP) and meso-tetra (4-sulfnato-phenyl)porphyrin (TPPS) were performed in solution. Metalporphyrincomplexation can be identified by shifts in the Q-bands which appear in the 500-700 nm range. The following solutions were tested: 10^{-3} M Nd^{3+} with 10^{-5} M TMPyP, 10^{-3} M Nd^{3+} with 10^{-5} M TPPS, and 0.0298 mg/ml UO_2^{2+} with 10^{-5} M TMPyP. However, shifts in the Q bands due to rare-earth complexation were not observed for these solutions.

Recent work on the development of "expanded porphyrin" molecules indicate that complexation with lanthanides and actinides can be achieved in solution due to the enlarged binding cavity. Other dyes have been used for the analysis of transition metals, such asphenylazoformic acid 2-phenylhydrazide with 1,5-diphenyl-carbazide (PAPDC) or Zincon tetra-octylammonium ion pair and catechols. Unlike porphyrins, these molecules have an open structure which may allow them to complex more readily to the lanthanides and actinides.

Reference

Klunder GL, Bürck J, Ache H-J, Silva RJ, Russo RE. Temperature effects on an evanescent field absorption sensor. (Submitted to *Appl. Spectrosc.*, August 1993).

*Lawrence Livermore National Laboratory

Bioorganometallic Chemistry: Bonding Studies of a (η^5-Pentamethylcyclopentadienyl)rhodium Aqua Complex to Nucleobases, Nucleotides, and Sequence-Specific Oligonucleotides for Human Genome Applications

R.H. Fish, D.P. Smith, M.F. Maestre, E. Kohen, M. Griffin, M.M Olmstead, B. Noll

The Organometallic Chemistry group has continued its studies on using an organorhodium aqua complex, $[Cp^*Rh(H_2O)_2(OTf)_2]_x$, to study its bonding modes with nucleobases, nucleotides, and sequence-specific oligonucleotides. These bonding studies were initiated to develop a new technique to anchor single DNA molecules to the glass and electrode surface of an epifluorescence microscope for potentially mapping and sequencing the human genome.

To develop this novel technique, we extensively studied the binding of water-soluble organometallic complexes to nucleobases, nucleosides, nucleotides, and sequence-specific oligonucleotides. For these purposes we used a water-soluble (η^5-pentamethylcyclopentadienyl)rhodium aqua complex and analyzed the structure of the metal-DNA base complexes using high-field nuclear magnetic resonance spectroscopy (NMR), circular dichroism (CD), FAB mass spectrometry (FAB-MS), Uv-Vis spectroscopy (Uv-vis), graphite furnace atomic absorption spectroscopy (GFAA) and, when possible, single-crystal x-ray analysis.

The reaction of the nucleobase, 1-methylcytosine, with a Cp*Rh(aqua) complex, $[\eta^5\text{-}Cp^*Rh(H_2O)_2(OTf)_2]_x$, **1**, provided two different complexes depending on the solvent media. Complex **3**, $[\eta^5\text{-}Cp^*Rh(\eta^1(N3)\text{-}1\text{-methylcytosine})_2.(H_2O)](OTf)_2$, was formed when acetone was used as the solvent; however, upon recrystallization of complex **3** from water (pH 5.1) or when using water as the reaction solvent, complex **4**, *trans*-$[\eta^5\text{-}Cp^*Rh(\eta^1(N3)\text{-}1\text{-methylcytosine})(\mu\text{-hydroxy})]_2(OTf)_2$, was isolated as a crystalline solid. The structures of **3** and **4** were verified by ^1H NMR, FAB/MS, elemental analysis, and in the case of **4**, by single-crystal x-ray analysis. Inspection of several bond lengths and angles of complex **4** indicates extensive intramolecular hydrogen bonding of the μ-OH groups with the exocyclic NH_2, 1.93(1) Å, and the 2-C=O group, 1.96(1) Å, whereas the angle between the NH_2-μ-O was found to be 149 (1) deg and that between the μ-OH-C=O being 155 (1) deg.

The reactions of adenosine 5'-monophosphate (5'-AMP) in water (pH 5-8) with a (η^5-pentamethylcyclopentadienyl)-rhodium aqua complex, $[Cp^*Rh(H_2O)_2(OTf)_2]_x$, **1**, showed, by ^1H and ^{31}P NMR spectroscopy, that the 5'-$P(O)_2$=O group significantly inhibited cyclic trimer formation, $[Cp^*Rh(\mu\text{-}\eta^1(N1):\eta^2(N6,N7)\text{-}5'\text{-AMP})]_3$, via competition with N1 and NH6 for the Cp*Rh site and, as well, provided other mononuclear and dinuclear Cp*Rh-O-P complexes. In contrast, both the phosphate methyl ester of 5'-AMP and 3'-AMP formed the cyclic trimer structures, $[Cp^*Rh(\mu\text{-}\eta^1(N1):\eta^2(N6, N7)\text{-methyl-}5'\text{-}/3'\text{-AMP})]_3$. The consequence of steric effects, as demonstrated by the position and substitution of the phosphate group attached to the ribose, on the diastereoselectivity of cyclic trimer formation, as observed by ^1H and ^{31}P NMR spectroscopy and circular dichroism analysis over time, shows that the phosphate methyl ester of 5'-AMP provides a greater diastereoselectivity (6:1) after one week of equilibration compared to 5'-AMP (1.5:1) and 3'-AMP (1.2:1).

The reactions of guanine derivatives, 9-ethylguanine (9-EG) and 9-methylhypoxanthine (9-MH), with *in situ* formed (η^5-pentamethylcyclopentadienyl)rhodium tris methanol complex, $[Cp^*Rh(CH_3OH)_3](OTf)_2$, reveals N7 bonding to the guanine nucleus. An x-ray structural study of $[Cp^*Rh(\eta^1(N7)\text{-}9\text{-MH})(\eta^1(O)\text{-}CH_3OH)_2](OTf)_2$, obtained from methanol, defined the exclusive N7 bonding to 9-MH (Rh-N7, 2.127 Å) and three additional hydrogen bonds of (1) a coordinated methanol ligand to C=O6 (CH_3OH—O=C, 1.83 Å), (2) the other coordinated methanol ligand to one of the triflate oxygens (CF_3SO_2O—$HOCH_3$, 1.86 Å), and (3) the other triflate anion to NH1 (CF_3SO_2O—HN, 1.89 Å). The pH profile of the $[Cp^*Rh(\eta^1(N7)\text{-}9\text{-MH})(\eta^1(O)\text{-}CH_3OH)_2](OTf)_2$ complex in water was also studied and showed a dramatic effect between pH 6-8 with an indication of N7, C=O6, and N1 bonding in the formation of an unusual and unprecedented cyclic trimer, $[Cp^*Rh(\mu\text{-}\eta^1(N1):\eta^2(C{=}O6,N7)\text{-}9\text{-MH})]_3(OTf)_3$, that was not detected with the Cp*Rh-9-EG complex. This result strongly suggests a significant steric effect of the NH_2 at C2 on the guanine nucleus inhibiting cyclic trimer formation.

We have also used ^1H NMR spectroscopy to initiate preliminary structural studies of an oligonucleotide, adenyl-3', 5'-adenosine (ApA). Preliminary results at several pH values reveal that only the 3' bonded adenine base binds Cp*Rh; downfield shift of the 3' H8 proton and not the 5' H8 proton, whereas neither the 3'or 5' H2 protons were found to be shifted. It is clear from these preliminary NMR results that ApA does not form trimers nor does it appear to form intrastrand complexes. Future studies on oligonucleotide reactions with the Cp*Rh aqua species will be an important focus.

Because the described human genome application depended on the selective binding of the sequence-specific oligonucleotide to the [Cp*Rh (Aqua)] complex, we emphasized these studies over the ApA studies described above. Structural studies on several sequence-specific oligonucleotides that may selectively interact with the [Cp*Rh(Aqua)] complex; *e.g.*, $(3'\text{-dA-}5')_{12}$ [*12-A*], (3'-dCCCGCCGCTGGA-5')] [*12-mer*], and the$(3'dA)_{12}$(dCCCGCC-GCTGGA-5') [*24-mer*]; were analyzed by CD, Uv-vis, and GFAA (Rh) analysis, after purification by dialysis.

Comparison of the CD spectra of the *24-mer*, *12-mer*, and the *12-A* oligomers, when reacted individually with the [Cp*Rh(Aqua)] complex at the molar ratios of one Cp*Rh/two base pairs, shows that the greatest change in the CD corresponds to the regions of the CD spectrum that are associated with the *12-A* oligomer structure. Interestingly, the largest alteration of the CD is found in the spectral regions below 260 nm in the *24-mer*, and similarly in the *12-A* oligomer. There are only small changes in the *12-mer* spectra upon addition of the [Cp*Rh(Aqua)] complex. The CD spectral studies are; therefore, indicative of changes mainly in the *12-A* oligomer section of the *24-mer*. This result agrees with the previous NMR binding studies of the [Cp*Rh(Aqua)] complex with the individual nucleobases, which indicated a strong binding preference for the adenine base.

Preliminary epifluorescence microscopy results, after annealing the Cp*Rh-*24-mer* complex with λ-DNA, have shown that a large fraction of the visualized single λ–DNA molecules are anchored to the electrode or glass

surfaces of the microscope stage. The anchored single λ-DNA molecules bond to one end with the implication that the anchor occurs via the Cp*Rh-*24-mer* complex binding to the terminus complimentary sequence of λ-DNA; *i.e.*, [Cp*Rh-*24-mer*-λ-DNA] and, as well, the open coordination sites on the Cp*Rh metal center also bind to both the glass and electrode surfaces. Future studies will be focused on the human genome application with experiments designed to cut the visualized λ-DNA with a laser (mapping), micromanipulation of the cut fragment, and amplification by PCR techniques for sequencing the DNA fragment; a novel technique to map and sequence the human genome.

References

Smith DP, Olmstead MM, Noll BC, Maestre MF, Fish RH. Bioorganometallic chemistry, 2. synthesis and structural studies of the reactions of a nucleobase, 1-methylcytosine, with a (η^5-pentamethylcyclopentadienyl)rhodium aqua complex. *Organometallics*, 1993; 12:593.

Smith DP, Kohen E, Maestre MF, Fish RH. Bioorganometallic chemistry, 3. role of the phosphate group during reactions of adenosine monophosphate derivatives with an (η^5-pentamethylcyclopentadienyl)-rhodium aqua complex in the diasteroselective formation of cyclic trimers, $[Cp^*Rh(AMP)]_3$. *Inorg. Chem.* 1993; 32: 4119.

Smith DP, Griffin M, Olmstead MM, Maestre MF, Fish RH. Bioorganometallic chemistry, 4. synthesis and structural studies of the reactions of a nucleobase, 1-methylcytosine, with a (η^5-pentamethylcyclopentadienyl)rhodium aqua complex. *Inorg. Chem.*, 1993, 32: 4677.

Removal and Recovery of Toxic Metal Ions from Aqueous Streams by Use of Polymer Pendant Ligands

R.H. Fish, S. Huang, W. Li , R.L. Albright, W. Fries

The Efficient Separation and Processing Integrated Program (ESPIP), Office of Technology Development, Office of Research and Development, of the overall DOE Environmental Management Program, has the mandate to develop technology for the separation and recovery of metal ions from various designated DOE integrated demonstration sites. The DOE/OTD (Resource Recovery Project) integrated demonstration project that focuses on the Berkeley Pit in Butte, Montana, will not only evaluate and test technologies for removal and recovery of both toxic and economically important metals, but also demonstrate the feasibility of various technologies for this integrated demonstration site, other sites in the United States and globally.

One important technology to be evaluated for ESPIP, polymer pendant ligands (more commonly named *ion-exchange resins*) that could have a profound effect on the removal and recovery of metals from the Berkeley Pit and other integrated demonstration sites, will be the focus of this new LBL-Rolm & Haas program on the separation needs for various toxic and economically significant metals found in the Berkeley Pit at pH 2.5. Selectivity of the polymer pendant ligands for each metal or several groups of metals such as Fe, Cu, Zn, Al, Mn, Hg, and Mg will be the key to the success of this important remediation technique for the Berkeley Pit and is the objective of our LBL program in collaboration with the Rohm and Haas research laboratories.

Material Applications

Development of New Composite Aerogel Materials

A.J. Hunt, W. Cao, D. Lee, L. Martin, S. Maxwell, M.S. Quinby-Hunt, X.Y. Song, P. Stevens, S.Q. Zeng

Aerogel materials are porous, low-density, nanostructured solids with many unique properties including low thermal conductivity, high transparency, high surface area, catalytic activity, and low sound velocity. This research is directed toward developing new nanocomposite aerogel materials for a number of applications. An important focus of the work in the past two years has been to substantially improve the thermal resistance of silica aerogel by adding nanophase carbon. Three primary benefits accrue from composite aerogel thermal insulation; extending the range of applications to higher temperatures, providing a more compact insulation for space-sensitive applications, and lowering the cost of the aerogel by as much as 30%. Superinsulating aerogel can replace existing CFC-containing polyurethane insulation and significantly improve the thermal efficiency of refrigerators and freezers, reduce heat losses in hot and cold piping, insulate batteries in electric vehicles, and reduce energy losses in a variety of industrial applications. Several Cooperative Research and Development Agreements (CRADAs) for the commercialization of aerogel-based materials are under discussion. Recently, the aerogel insulation research was generalized to the wider area of nanostructured aerogel composites. A number of new materials with unusual properties attributable to their very fine dimensions (such as quantum-size effects) were prepared. These materials may be useful for magnetic cooling cycles, electroluminescent displays, and optical devices.

Thermal Insulation Research

The thermal insulation work concentrated on developing composites with smaller pore size to improve the

pressure versus thermal resistance performance, determining optimum carbon doping levels for various applications, modeling the thermal conductivity in aerogels (Zeng et al., 1993) and designing and building a new instrument to measure the pressure and temperature dependence of aerogel's thermal conductivity.

In evacuated silica aerogel at ambient temperatures, infrared radiation is responsible for up to half or more of its thermal conductivity; therefore, reducing the radiation substantially improves the thermal performance of aerogel insulation. At elevated temperatures (200 to 500°C), the radiative component of heat transfer in aerogel becomes dominant and must be suppressed. This radiation can be blocked by adding a finely dispersed material with a high absorption coefficient. In earlier work, carbon particles were added to the aerogel at the sol or liquid stage and subsequently processed and dried. Measurements showed an increase of more than 50% in thermal resistance at ambient temperatures and much larger percentage increases at higher temperatures.

However, the addition of carbon at the formulative stage of the gel coincidentally reduced the strength of the aerogel. As a result of research conducted to address this limitation, we discovered and are developing a new method to add carbon that has many advantages over the method in which particles are added in the sol or liquid stage. A true nanocomposite aerogel is created by the process of chemical vapor infiltration (CVI), when aerogel is infiltrated with a gas that is catalytically decomposed by the aerogel. This method increases the strength of the aerogel composite and allows for doping levels several times the original mass of silica. We have explored a variety of gases for CVI deposition of carbon. Infrared and surface area measurements along with high-resolution transmission electron microscopy were used to characterize the composites. Patent applications covering the CVI-aerogel nanocomposite production process are being filed.

To assess the thermal performance of composite aerogel insulation, we designed and built an instrument to measure the thermal conductivity of aerogel as a function of pressure and temperature. A thin-film-heater thermal conductivity apparatus with variable pressure capabilities is nearing completion. To analyze and predict the thermal performance of aerogel, the heat transfer due to the radiation, conduction, and gas conductivity and their interaction inside aerogel is being modeled. The objective is to predict the thermal conductivity as a function of temperature and gas pressure. The predicted effects of carbon doping on the thermal performance of aerogel are quite dramatic at temperatures from 200 to 500°C and, if borne out, opacified aerogel will be an outstanding insulating material for temperatures up to 500°C.

Development and Exploration of New Nanocomposite Materials

We have developed techniques for the preparation of a whole new family of unique nanoporous composite materials based on CVI-aerogel and other preparation techniques. In addition to achieving high densities of carbon in the silica aerogel, nanophase composites were prepared using elemental silicon and iron. Composites of silica aerogels and the oxides of iron, nickel, and copper were also synthesized. Transmission electron microscopy was used extensively to characterize the nanostructure and crystallinity of the new composites. Using these methods, we believe that a wide variety of new composite materials can be produced. Such nanophase materials have potential applications in magnetic cooling cycles, electroluminescent displays, and for transparent magnetic materials. Silicon-silica composites exhibit photoluminescence that our measurements confirm is due to quantum well confinement effects (Cao and Hunt, 1993). These materials may well be useful for electroluminescent display devices. The iron and iron oxide composites exhibit magnetic properties that appear useful for magnetic cooling cycles.

References

Cao W and Hunt AJ. Thermal annealing of photoluminescent Si on silica aerogels. (submitted to *Applied Physics Letters*, September 1993)

Zeng SQ, Hunt AJ, Cao WQ, Greif R. Pore size distribution and gas phase thermal conductivity of silica aerogel. (submitted to *Journal of Heat Transfer*, September 1993)

Modeling Light Scattering from Nonspherical Microorganisms in the Ocean

A.J. Hunt, P. Hull, M.S. Quinby-Hunt, D.B. Shapiro, F. Shaw

The goal of this project is to investigate and predict the optical properties of ocean water by modeling and measurement of the light scattering from ensembles of nonspherical marine microorganisms. The results of this investigation can be used to evaluate the effects of this scattering on visibility, irradiance, and transmission of polarized and unpolarized light in the ocean. The project also investigates the interaction of polarized light with optically active unicellular marine organisms with chiral structure in order to clarify the causes and effects of polarized light in the ocean.

The Mueller matrix scattering formalism is used to characterize and compare the experimental and theoretical results. Approximate analytical methods were developed to predict the Mueller matrices for light scattered from variously-shaped particles as analogs for complex biological structures. Analytical methods were used to investigate the effects caused by the orientation of ensembles of nonspherical particles, and to determine the feasibility of detecting orientation by measuring Mueller scattering matrix elements that are zero only for nonoriented ensembles. To develop analytical tools to study light scattering from nonspherical particles, model systems were chosen for measurement and modeling of the scattering from helical and ellipsoidal particles.

Simple Helical Systems: Sperm Heads of *Eledone cirrhosa*

The sperm head from the octopus *Eledone cirrhosa* was chosen as the model

system for a helical scatterer (Shapiro et al., 1993a,b), because it is physically well-characterized, and is known to affect circularly polarized light. Light scattering measurements were used to establish the angular dependence of the Mueller matrix elements of this system. The measurements were compared to calculations from several different approximations [a first Born approximation for a continuous helix, a first Born approximation for a helix constructed of non-interacting dipoles, and the coupled-dipole approximation] as no rigorous solutions were available. Each of the various approximations showed general agreement with the experimental results, however, they each were found to have advantages and disadvantages.

The coupled-dipole model is the most rigorous solution; however, only the scattering from a helix whose pitch and radius are less than the wavelength of light can be calculated accurately at present—given the capacity of current supercomputers. Nonetheless, the coupled-dipole approximation must be used when modeling helical structures which are thick or have a high relative dielectric constant. A helix that is the thickness of the order of the wavelength of light must be modeled with several strands which increases the computational power required for the calculation.

For thin helices whose pitch and radius are comparable to the wavelength of light, the first Born approximations were found to be of value particularly for calculating the matrix element which describes the depolarization of circularly polarized light. Due to theoretical limitations, some other Mueller matrix elements cannot be calculated using the first Born approach. So many subunits are necessary to apply the noninteracting dipole model that limitations of current supercomputers restrict its use and the continuous model often calculates matrix elements that are closer to the experimental results.

Complex Helices: A Plectonemic Helix

A more complex shape, a plectonemic helix (a closed helix with multiple twists; this shape appears in bacteria and other organisms) was also modeled using a coupled-dipole approximation (Shapiro et al., 1993c). This shape was chosen to test whether the available models and computers were capable of calculating scattering from a system more complex than the single-twisted helix used to describe the octopus sperm head. A mathematical model of a plectonemic helix was developed. Each base-pair of the idealized plectonemic helix was represented by a single dipole. The polarizability at each dipole can be defined with respect to the contour describing the helix. The scattering averaged over all orientations was calculated using a numerical technique based the Gaussian-Legendre method at several wavelengths. These calculations illustrate that the coupled-dipole approximation is useful in describing polarized-light scattering from a complex structure.

Ellipsoids: Spores of *Bacillus subtilis*

Light scattering was also measured from ellipsoidal bacterial spores of *Bacillus subtilis* that are present in the ocean. Samples of Bacillus subtilis (grown under conditions of synchronous growth until sporulation) were prepared and scattering was measured at wavelengths of 488 and 633 nm. Observed Mueller matrix elements from the ellipsoidal bacterial spores differed significantly from those of spheres of comparable size. Scattering was wavelength dependent. Micrographs were used to provide a preliminary description of the spores, which will be used as the basis for calculations of the Mueller matrix elements using the coupled-dipole approximation. The coupled-dipole approach is being developed in conjunction with Dr. P. Hull at Tennessee State University.

References

Shapiro DB, Maestre MF, Hull PG, McClain WM, Shi Y, Quinby-Hunt MS, Hearst JE, Hunt AJ. 1993a. Determination of the average orientation of DNA in the octopus sperm, *Eledone cirrhosa*, using polarized light scattering. (accepted for publication, *AppliedOptics*, 1993)

Shapiro DB, Hull PG, Shi Y, Maestre MF, Quinby-Hunt MS, Hearst JE, Hunt AJ. 1993b. Toward a working theory of polarized-light scattering from helices. (in press, *J. Chem. Phys.*, 1993).

Shapiro DB, Hull PG, Hunt AJ, Hearst JE. 1993c. Calculations of the Mueller scattering matrix for a DNA plectonemic Helix. (accepted for publication, *J. Chem. Phys.*; work originally presented at *X-Ray Physics Gordon Research Conference*, Colby-Sawyer College, New London, NH, August 9-13, 1993.

Mueller Matrix Measurements of Sea Ice

A.J. Hunt, D. Miller, M.S. Quinby-Hunt

The goal of this work is to identify and characterize the polarization aspects of light scattered from sea ice. To this end, we are studying light scattered by sea ice in the laboratory, determining possible polarization signatures presented by the ice, and designing and deploying an instrument specially tailored to probe the polarization characteristics of sea ice *in situ*. Sea ice is a complex, heterogeneous material that exhibits strong polarization-dependent scattering, which can be fully described by the 4×4 Mueller scattering matrix. A complete description of the angle-dependent scattering and polarization properties of sea ice does not exist in the literature. Such a description is an essential ingredient of realistic models for radiative transfer through the ice and interpretation of satellite data on ice-pack characteristics.

An instrument is being developed which will provide measurement of angle-dependent Mueller matrix elements with visible light for ice samples grown in the lab as well as for core samples of sea ice. These measurements will form the basis of understanding light scattering in sea ice at a laboratory scale. In addition, we are developing a portable instrument for *in situ* measurements of various types of sea ice.

Laboratory work involves using an existing polarization-modulated angle-scanning nephelometer with a sample stage that can be cooled below the eutectic temperature of sea-ice brine (-23°C). Light scattering will be measured from small cylinders and slabs of ice to investigate several of the matrix

elements believed to be most sensitive to ice characteristics such as bubble and brine pocket structure, crystal orientation, and temperature. A cold stage was designed and built for the existing nephelometer. Techniques for large crystal sea ice sample preparation were developed, samples simulating sea ice were grown in the laboratory, and preliminary optical measurements of the samples were made.

To make measurements in the field, a novel, field-deployable nephelometer is being developed for use in the Arctic. This instrument will be used to make *in situ* measurements of the polarization-dependent scattering of sea ice at visible wavelengths. A design for a bistatic *in situ* nephelometer based on the laboratory-based polarization-modulation instrument has been developed. The Russian Arctic facilities at Zhokov Island were visited and considered for use as an access point for potential field sites. This site has accessible nilas, stable polynya, new ice, pack ice, leads and pressure ridges. This appears to be an excellent potential site for *in situ* measurements of a variety of types of Arctic sea ice.

The laboratory and field results will be used to enhance the understanding of the scattering and polarization properties of sea ice. The data will be useful in modeling efforts to understand light propagation in sea ice. This understanding can be applied to the results of remote sensing techniques to provide important information regarding issues such as ice formation, ice thickness, melting, and effects on shipping, wildlife, and climate change.

Sponsors

Support from the following sources was provided through the U.S. Department of Energy under Contract No. DE-AC03-76SF00098

- U.S. Department of Energy
  - Assistant Secretary for Energy Efficiency and Renewable Energy:
    - Office of Transportation Technologies, Electric and Hybrid Propulsion Division
    - Office of Industrial Technologies:
      - Office of Industrial Processes
      - Advanced Industrial Concepts Division, Advanced Industrial Concepts Materials Program
    - Office of Energy Research:
      - Office of Basic Energy Sciences, Chemical Sciences Division
      - Office of Health and Environmental Research, Medical Applications and Biophysical Research Division
  - Assistant Secretary for Environmental Restoration and Waste Management:
    - Office of Technology Development, Office of Research and Development
  - Assistant Secretary for Fossil Energy:
    - Office of Coal Utilization, Advanced Research and Technology Development, Division of Surface of Coal Gasification, Morgantown Energy Technology Center
  - Office of Naval Research, Ocean, Atmosphere, and Space and Technology Department
- Lawrence Berkeley Laboratory, Laboratory-Directed R&D Funds
- Lawrence Livermore National Laboratory Contract No. W-7405-ENG-48
- United States Advanced Battery Consortium

Energy & Environment Division
Lawrence Berkeley Laboratory
University of California
Berkeley, CA 94720